SpringerBriefs in Applied Sciences and Technology

Micromagnetics and Recording Materials

Bearbeitet von
Dan Wei

1. Auflage 2012. Taschenbuch. viii, 110 S. Paperback
ISBN 978 3 642 28576 9
Format (B x L): 15,5 x 23,5 cm
Gewicht: 195 g

Chapter 2
Maxwell Equations and Landau–Lifshitz Equations

Abstract This chapter will present the theoretical, mathematical and computational fundamentals for micromagnetics. The target of micromagnetics is to clarify the motion of magnetic moments in ferromagnetic materials and devices, which is described by the nonlinear Landau–Lifshitz equations, or the equivalent Landau–Lifshitz–Gilbert (LLG) equations. In the LLG equations, the time derivative of the magnet moment in a micromagnetic cell is controlled by the local effective magnetic field. The effective magnetic field contains the terms determined by the fundamental and applied magnetism in a magnetic material, including the external field, the crystalline anisotropy field, the exchange field, the demagnetizing field, and the magneto-elastic field. Among these field terms, the most time-consuming one in computation is the demagnetizing field, which will be calculated by the Green's function method following the Maxwell's equations.

Keywords Maxwell equations · Vector analysis · Demagnetizing matrix · Free energy · Landau–Lifshitz equations · History of micromagnetics

The development of micromagnetics was related to the computational science in an unusual way. In 1945, the great mathematician John von Neumann started a computer project in Princeton, to redesign the logic structure of the first computer ENIAC invented in 1944 by J. Presper Eckert and John Mauchly. Neumann brought up the idea of "program digital computer", including a processing unit, a data and program memory, a controller and an input/output device. The major problem in ENIAC was the lack of memory; thus Neumann suggested to build up a memory by vacuum tubes, and made the independent development of hardware and software possible. The storage capacity of vacuum tube memory was limited; therefore a magnetic recording tape drive "Uniservo" was built up as the external memory of the UNIVAC computer in 1948 by the first computer company Eckert–Mauchly Computer Corporation (EMCC). In 1945, Neumann already saw the great potential of computer to change the way of mathematical computation, especially for the nonlinear problems. At the heart of micromagnetics, there is such a nonlinear problem

D. Wei, *Micromagnetics and Recording Materials*, SpringerBriefs in Applied Sciences and Technology, DOI: 10.1007/978-3-642-28577-6_2,

defined by the Landau–Lifshitz (LL) equations [1]; only after using the computational methods by Brown in 1960s [2], micromagnetics finally became dependable and served as the basic theory in magnetic recording industry.

The target of micromagnetics is to clarify the motion of magnetic moments in ferromagnetic materials and devices, which is described by the LL equations, or the equivalent Landau–Lifshitz–Gilbert (LLG) equations. In the LLG equations, the time derivative of the magnet moment $\hat{m}$ in a micromagnetic cell is controlled by the local effective magnetic field $\mathbf{H}_{\text{eff}}$, which varies along with $\hat{m}(\mathbf{r})$ and forms a high nonlinearity. The effective magnetic field $\mathbf{H}_{\text{eff}}$ contains the terms determined by the fundamental and applied magnetism, including the external field, the crystalline anisotropy field, the exchange field, the demagnetizing field, and the magneto-elastic field. Among these field terms, the most time-consuming one in computation is the demagnetizing field, which will be calculated by the Green's function method following the Maxwell's equations.

2.1 Maxwell Equations and Vector Analysis

In Maxwell's book *A Treatise on Electricity and Magnetism* [3], all equations of electromagnetic field were written in the component form. Similar to the mathematical development after Newtonian mechanics in the eighteenth century, there was also a period of mathematics development after Maxwell's equations. In late nineteenth century, Josiah Willard Gibbs and Oliver Heaviside developed the vector analysis, and Maxwell's equations were rewritten in the vector form, which is beautiful and even looks like an apocalypse, as commented by Laue [4].

Gibbs was awarded the first Ph.D. in Engineering in the US from Yale in 1863. He went to Europe in 1866, and spending a year each at Paris, Berlin, and Heidelberg. Maxwell's theory published in 1865 predicted the existence of electromagnetic waves moving at the speed of light. Hermann von Helmholtz was at Heidelberg at that time, and he was one of the first physicists in continental Europe who was interested in Maxwell's theory. Gibbs was influenced by Helmholtz's interests during his visit. In 1879, Helmholtz suggested his student Heinrich Hertz to test experimentally the Maxwell's theory of electromagnetism, which was finally done by Hertz later in 1886. In the same period, Gibbs invented vector analysis in Yale, and developed a theory of optics using his notation.

Oliver Heaviside, another independent inventor of vector analysis, abstracted Maxwell's set of equations to four equations in the vector form. Heaviside was a self-taught English electrical engineer, mathematician, and physicist. In 1873 Heaviside had encountered Maxwell's newly published book [3]. He felt it was great, greater and greatest with prodigious possibilities in its power, and determined to master the book. However he had no knowledge of mathematical analysis at that time. Finally in 1884, Heaviside reformulated Maxwell's 20 equations in 20 unknowns to the four vector equations using vector calculus. Those four vector equations,

involving abstract mathematical terminology as curl and divergence, are formally called as "Maxwell's equations".

2.1.1 Vector Analysis

The first step to solve a problem is to describe the space of the object. A coordinate system has to be introduced for the mathematical expressions of physical quantities. The Cartesian coordinate is an universal choice, and especially suitable for numerical calculations. In an n-dimensional space, the position vector is $\mathbf{r} = (x_1, x_2, ..., x_n)$ and an arbitrary vector has the form $\mathbf{A} = (A_1, A_2, ..., A_n)$, which can be easily stored in an n-dimensional array in computer. It just has to be remembered, in the numerical calculation, a step size has to be introduced for a component x_i; otherwise the memory of the position vector will be infinite. Actually this discretization is a basic problem in micromagnetics, which will be further discussed in Chap. 4.

In micromagnetics, the magnetization $\mathbf{M}$ takes the role of position vector in mechanics. The polar coordinate expression $\mathbf{M} = (M, \theta, \phi)$ of magnetization is often used, where the inclination angle $0 \leq \theta \leq \pi$ and the azimuth angle $0 \leq \phi < 2\pi$. The real polycrystalline material is complicated, usually including multilevel of microstructure and different orientation of crystal, therefore the coordinate transformation between Cartesian and polar coordinate of the same vector is important:

$$\begin{aligned} M_1 &= M \sin\theta \cos\phi, \\ M_2 &= M \sin\theta \sin\phi, \\ M_3 &= M \cos\theta. \end{aligned} \tag{2.1}$$

$$\begin{aligned} M &= \sqrt{M_1^2 + M_2^2 + M_3^2}, \\ \theta &= \cos^{-1}\left(M_3/M\right), \\ \phi &= \begin{cases} \cos^{-1}\left(M_1/\sqrt{M_1^2 + M_2^2}\right) & (M_2 > 0) \\ -\cos^{-1}\left(M_1/\sqrt{M_1^2 + M_2^2}\right) & (M_2 < 0). \end{cases} \end{aligned} \tag{2.2}$$

The accurate definitions of scalar, vector and tensor depend on the characteristics of the quantity under the rotation of coordinate system. The scalar is invariant under rotation; the vector is transformed by the rotation matrix under rotation; and the tensor is transformed by two or more rotation matrices, depending on its order.

There are two rotation matrix $\tilde{R}$ and $\tilde{R}_{\mathrm{E}}$ introduced here: $\tilde{R}$ is related to two angles θ and ϕ, which is not universal but enough in most of cases; and $\tilde{R}_{\mathrm{E}}$ is general and related to three Euler angles α, β and γ, as defined in Fig. 2.1. The rotational property of a vector $\mathbf{v}$ can be described by two angles: first the coordinates (x, y, z) rotates around y-axis by angle θ, then rotates around the old z-axis by angle ϕ, as seen in Fig. 2.1a. The unit vectors $\hat{e}'_\alpha$ of the new coordinates are transformed from $\hat{e}_\alpha$ of the

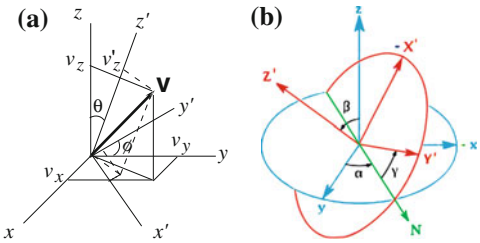

Fig. 2.1 Rotation of Cartesian coordinates. **a** Two angles, no self rotation; **b** Euler angles

old coordinates as $\hat{e}'_\alpha = \tilde{R} \cdot \hat{e}_\alpha$ by a rotation matrix $\tilde{R}$:

$$\begin{aligned}\tilde{R} &= \begin{pmatrix} \cos\phi & -\sin\phi & 0 \\ \sin\phi & \cos\phi & 0 \\ 0 & 0 & 1 \end{pmatrix} \begin{pmatrix} \cos\theta & 0 & \sin\theta \\ 0 & 1 & 0 \\ -\sin\theta & 0 & \cos\theta \end{pmatrix} \\ &= \begin{pmatrix} \cos\theta\cos\phi & -\sin\phi & \sin\theta\cos\phi \\ \cos\theta\sin\phi & \cos\phi & \sin\theta\sin\phi \\ -\sin\theta & 0 & \cos\theta \end{pmatrix} \end{aligned} \tag{2.3}$$

The components (v'_1, v'_2, v'_3) of a fixed vector $\mathbf{v}$ in the new coordinate system is related to (v_1, v_2, v_3) in the old coordinate system by the inverse rotation matrix or transpose of rotation matrix $\mathbf{R}^{\mathrm{T}}$, in a passive ("pose") manner:

$$v'_i = R^{\mathrm{T}}_{ij} v_j = R_{ji} v_j \quad (i = 1, 2, 3;\ j = 1, 2, 3), \tag{2.4}$$

$$v_i = R_{ij} v'_j \qquad (i = 1, 2, 3;\ j = 1, 2, 3), \tag{2.5}$$

where the Einstein notation (auto sum over dummy indices) is used. Equations (2.4) and (2.5) can be viewed as the accurate definition of a vector.

When the rotation matrix $\tilde{R}_{\mathrm{E}}$ of Euler angles is utilized to define vectors, the transform between the new components (v'_1, v'_2, v'_3) and old components (v_1, v_2, v_3) is in an active ("displacement") manner, with rotations α (around z), β (around N or y' with $\gamma = 0$) and γ (around z') successively:

$$\mathbf{v}' = \tilde{R}_{\mathrm{E}} \cdot \mathbf{v}, \quad v'_i = R^{ij}_{\mathrm{E}} v_j \tag{2.6}$$

where the transpose of $\tilde{R}_{\mathrm{E}}$ related to the definition of Euler angles in Fig. 2.1b [this definition is different from the most common definition of Euler angles with a transform $x \leftrightarrow y$ for compatibility with Eq. (2.3)] is defined as:

$$\tilde{R}_{\mathrm{E}}^{\mathrm{T}} = \begin{pmatrix} c_\alpha & -s_\alpha & 0 \\ s_\alpha & c_\alpha & 0 \\ 0 & 0 & 1 \end{pmatrix} \begin{pmatrix} c_\beta & 0 & s_\beta \\ 0 & 1 & 0 \\ -s_\beta & 0 & c_\beta \end{pmatrix} \begin{pmatrix} c_\gamma & -s_\gamma & 0 \\ s_\gamma & c_\gamma & 0 \\ 0 & 0 & 1 \end{pmatrix}$$
$$= \begin{pmatrix} c_\alpha c_\beta c_\gamma - s_\alpha s_\gamma & -c_\alpha c_\beta s_\gamma - s_\alpha c_\gamma & c_\alpha s_\beta \\ s_\alpha c_\beta c_\gamma + c_\alpha s_\gamma & -s_\alpha c_\beta s_\gamma + c_\alpha c_\gamma & s_\alpha s_\beta \\ -s_\beta c_\gamma & s_\beta s_\gamma & c_\beta \end{pmatrix} \tag{2.7}$$

where c stands for cosine and s stands for sine functions respectively. Equation (2.7) is equivalent to Eq. (2.3) if we let $\alpha = \phi$, $\beta = \theta$ and $\gamma = 0$, as stated in Fig. 2.1.

There are three kinds of operations between two vectors: dot product, cross product and diad, where the results are scalar, vector and matrix, respectively:

$$\mathbf{A} \cdot \mathbf{B} = A_i B_i = A_1 B_1 + A_2 B_2 + A_3 B_3; \tag{2.8}$$
$$\mathbf{A} \times \mathbf{B} = \begin{vmatrix} \hat{e}_1 & \hat{e}_2 & \hat{e}_3 \\ A_1 & A_2 & A_3 \\ B_1 & B_2 & B_3 \end{vmatrix} = \hat{e}_i \varepsilon_{ijk} A_j B_k; \tag{2.9}$$
$$\left(\mathbf{A}\mathbf{B}^{\mathrm{T}}\right)_{ij} = A_i B_j, \tag{2.10}$$

where $\hat{e}_1, \hat{e}_2, \hat{e}_3$ are the unit vectors along x, y, z axes in Cartesian coordinates, respectively. The ε_{ijk} is a third-order antisymmetric tensor with only 6 nonzero elements $\varepsilon_{123} = \varepsilon_{231} = \varepsilon_{312} = 1 \ = -\varepsilon_{321} = -\varepsilon_{213} = -\varepsilon_{132}$.

The operation related to scalar is easy, just a simple multiplication. For the tensors, there are an operation called contraction: the contraction between the Nth-order tensor and the Mth-order tensor is a $|N-M|$th-order tensor:

$$X_{i_1 i_2 \ldots i_N} Y_{i_1 i_2 \ldots i_M} = Z_{i_{M+1} i_{M+2} \ldots i_N} \quad (N \geq M). \tag{2.11}$$

Therefore, the sum over dummy indices using Einstein notations is a kind of contraction, as seen in Eqs. (2.8) and (2.9). The trace of a matrix $\tilde{X}$ is a contraction between $\tilde{X}$ and the unit matrix or Kronical-delta function:

$$X_{i_1 i_2} \delta_{i_1 i_2} = X_{i_1 i_1}, \tag{2.12}$$

where the zeroth-order tensor is just a scalar; and X_{ii} is the trace of $\tilde{X}$.

As we stated before, the rotational characteristics of vector and tensor are different. If the passive and active manner of the rotation defined in Eq. (2.3) of angles θ and ϕ and Eq. (2.7) of Euler angles are used respectively, after rotation, the diad $\tilde{X} = \mathbf{A}\mathbf{B}^{\mathrm{T}}$ has the same characteristics as a tensor:

$$\tilde{X}' = (\tilde{R}^{\mathrm{T}}\mathbf{A})(\tilde{R}^{\mathrm{T}}\mathbf{B})^{\mathrm{T}} = \tilde{R}^{\mathrm{T}} \tilde{X} \tilde{R}$$
$$\tilde{X}' = (\tilde{R}_{\mathrm{E}}\mathbf{A})(\tilde{R}_{\mathrm{E}}\mathbf{B})^{\mathrm{T}} = \tilde{R}_{\mathrm{E}} \tilde{X} \tilde{R}_{\mathrm{E}}^{\mathrm{T}}. \tag{2.13}$$

These characteristics under rotation is very useful when we calculate the demagnetizing matrices of micromagnetic cells in a thin film or a device.

The Maxwell equations include the differentiation of electric and magnetic vector fields **E** and **B** in three-dimensional (3-D) space. When the vector analysis is applied to calculus in space, the differentiation in one-dimension becomes the gradient operator in three-dimensions. The express of the gradient operator ∇ and the Laplace operator ∇^2 depends on the coordinate system. In Cartesian coordinates $\hat{e}_1, \hat{e}_2, \hat{e}_3$ are constant vectors, but in cylindrical coordinates two out of three local unit vectors $\hat{e}_\rho, \hat{e}_\phi$ vary with position **r**, and in spherical coordinates all three local unit vectors $\hat{e}_r, \hat{e}_\theta, \hat{e}_\phi$ vary with **r**. Thus when the ∇ is acting on a vector $\mathbf{A} = \hat{e}_i A_i$ it is much more complicated in cylindrical and spherical coordinates.

In this book, we will just use Cartesian coordinates to build up the regular mesh of micromagnetic cells, therefore things become much easier. When the gradient operator acts on a vector, there are also three kinds of differentiation operations: dot product (divergence), cross product (curl) and diad:

$$\nabla = \hat{e}_i \partial_i = \hat{e}_x \frac{\partial}{\partial x} + \hat{e}_y \frac{\partial}{\partial y} + \hat{e}_z \frac{\partial}{\partial z} \tag{2.14}$$

$$\nabla \cdot \mathbf{A} = \partial_i A_i = \frac{\partial A_x}{\partial x} + \frac{\partial A_y}{\partial y} + \frac{\partial A_z}{\partial z}, \tag{2.15}$$

$$\nabla \times \mathbf{A} = \hat{e}_i \varepsilon_{ijk} \partial_j A_k, \tag{2.16}$$

$$\left(\nabla \mathbf{A}^{\mathrm{T}}\right)_{ij} = \partial_i A_j. \tag{2.17}$$

The operations between two ∇ operators (if we let $\mathbf{A} = \nabla$) can also be performed. The dot product of two ∇ is the famous Laplacian ∇^2, which is a scalar operator; the cross product of two ∇ is zero when it acts on a scalar field; and the diad of two ∇ often appears in the calculation of demagnetizing matrix.

2.1.2 Maxwell's Equations

The development of electromagnetism in the eighteenth and nineteenth centuries has been reviewed in Sect. 1.1. In 1861–1862, inspired by Faraday's thought of electromagnetic induction in dielectrics, Maxwell brought up the concept of "displacement current" in his paper "On Physical Lines of Force", and he added this extra term of effective current in the Ampere's law. In his book *A Treatise on Electricity and Magnetism* finally published in 1873, the "general equations of electromagnetic field" were derived and discussed in electric and magnetic media, and the system of units were close to the cgs units, except that the speed of light c did not appear as in the modern form of the Maxwell's equations:

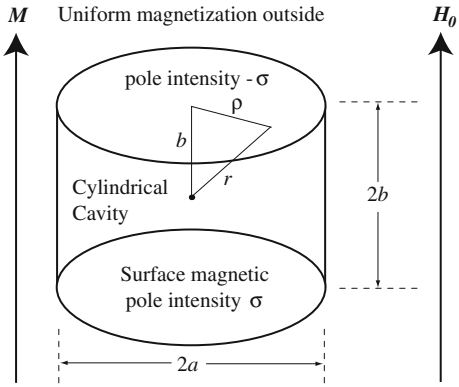

Fig. 2.2 Definition of magnetic induction **B** or magnetic field **H** by Maxwell: the force acting on an unit dipole at the center of cavity if $b \ll a$ or $b \gg a$, respectively

$$\nabla \cdot \mathbf{D} = 4\pi\rho_0, \tag{2.18}$$

$$\nabla \cdot \mathbf{B} = 0, \tag{2.19}$$

$$\nabla \times \mathbf{E} = -\frac{1}{c}\frac{\partial \mathbf{B}}{\partial t}, \tag{2.20}$$

$$\nabla \times \mathbf{H} = \frac{4\pi}{c}\mathbf{j}_0 + \frac{1}{c}\frac{\partial \mathbf{D}}{\partial t}, \tag{2.21}$$

where ρ_0 and $\mathbf{j}_0$ are the charge density and current density of free charge. The Coulomb's law in Eq. (2.18) was given in Sect. 77 of Maxwell's book; the Faraday's law of electromagnetic induction in Eq. (2.20) was derived in Sect. 598 by introducing the magnetic vector potential; the Gauss' law for magnetism in Eq. (2.19) was stated in Sect. 604; and the Ampere's law with the modification of displacement current in Eq. (2.21) was finally discussed in Sects. 607–610 [3].

There are four electromagnetic field in the Maxwell's equations in media: the electric displacement **D**, electric field **E**, magnetic induction **B** and magnetic field **H**; therefore the Maxwell's equations have to be solved self-consistently with the polarization equation of dielectrics in Eq. (1.4), the magnetization equation of magnetic media in Eq. (1.5), and the Ohm's law of conductors in Eq. (1.6).

The relationships among **B**, **H** and magnetization **M** of magnetic materials are actually the central topic of this book. When Maxwell introduced the magnetization equation of magnetic media in Sects. 395–400 [3], the magnetic induction **B** and magnetic field **H** were defined following Fig. 2.2. If there is a cylindrical cavity in an uniform magnetic medium with magnetization **M**, and the axis of the cylinder is parallel to **M**, the magnetic induction **B** is the force acting on the unit magnetic dipole at the center when the cavity is extremely flat ($b \ll a$), and the magnetic field **H** is the force on unit dipole when the cavity is extremely thin and long ($b \gg a$). The effective magnetic field (Maxwell called it "force" [3]) acting on the unit magnetic dipole can be found by a simple integration, by considering the contributions of the effective surface magnetic pole intensity $\pm\sigma = \pm M$ on the bottom/top surface:

$$F_z = H_0 + 2\int_0^a \frac{\sigma b\, 2\pi\rho \mathrm{d}\rho}{\left(\rho^2 + b^2\right)^{3/2}} = H_0 + 4\pi\sigma b \int_b^{\sqrt{a^2+b^2}} \frac{r\mathrm{d}r}{r^3}$$
$$= H_0 + 4\pi\sigma\left(1 - \frac{b}{\sqrt{a^2+b^2}}\right), \tag{2.22}$$

where $\mathbf{H}_0$ is an uniform external magnetic field, and the "force" $\mathbf{F} = F_z\hat{e}_z$ is along the z-axis or axis of the cylinder. In a flat cavity ($b \ll a$), $\mathbf{F} = \mathbf{H}_0 + 4\pi\mathbf{M}$ just equals the magnetic induction $\mathbf{B}$; in a long cavity ($b \gg a$), $\mathbf{F} = \mathbf{H}_0$ equals the magnetic field $\mathbf{H}$, because there is no other terms such as the exchange field acting on the unit dipole. These definitions of $\mathbf{B}$ and $\mathbf{H}$ are related to the demagnetizing field in magnetic media, which will be further discussed in the next section.

The experimental verifications of Maxwell's equations have been performed at a large scale, from microscopic to macroscopic. The electromagnetic field of fundamental particles in vacuum is micro-electric field $\mathbf{e}$ and micro-magnetic field $\mathbf{h}$. The electric field $\mathbf{E}$ and magnetic induction $\mathbf{B}$ in Maxwell's equations in media from Eq. (2.18) to Eq. (2.21) are actually the statistical average of the microscopic electromagnetic field $\mathbf{e}$ and $\mathbf{h}$ in an element of media:

$$\mathbf{E} = \langle\mathbf{e}\rangle_{\text{element}}, \quad \mathbf{B} = \langle\mathbf{h}\rangle_{\text{element}}. \tag{2.23}$$

The average is necessary because, microscopically, the atoms are vibrating, the electrons are moving; therefore the micro-electric field $\mathbf{e}$ and micro-magnetic field $\mathbf{h}$ are highly nonuniform in time and space. In the studies of macroscopic electric or magnetic materials, these fluctuations of microscopic electromagnetic field around fundamental particles need not to be considered, thus an average in an element, at least with a size of several conventional unit cells, can be made to obtain the macroscopic $\mathbf{E}$ and $\mathbf{B}$. However, if the scattering of external particle or wave with the matter has to be considered, quantum excitation, absorbing or emission processes are involved, the average in Eq. (2.23) is no longer appropriate.

The Maxwell's equations in vacuum have an beautiful symmetric form between electric and magnetic phenomena, except that there is no intrinsic "magnetic charge" for fundamental particles:

$$\nabla \cdot \mathbf{e} = 4\pi\rho, \tag{2.24}$$
$$\nabla \cdot \mathbf{h} = 0, \tag{2.25}$$
$$\nabla \times \mathbf{e} = -\frac{1}{c}\frac{\partial \mathbf{h}}{\partial t}, \tag{2.26}$$
$$\nabla \times \mathbf{h} = \frac{4\pi}{c}\mathbf{j} + \frac{1}{c}\frac{\partial \mathbf{e}}{\partial t}. \tag{2.27}$$

The concepts of polarization $\mathbf{P}$ and magnetization $\mathbf{M}$ do not exist microscopically, because the microscopic view is a view of elementary particles in vacuum. Therefore Eqs. (2.24)–(2.27) are enough to solve the microscopic electromagnetic field if the

sources $(\rho, \mathbf{j})$ of particles are known. In early twentieth century, Dutch physicist Hendrik Antoon Lorentz pointed out that, when the interactions among the electromagnetic field and fundamental particles are considered, there must be a formula for electromagnetic force to make the problem complete. This is the famous Lorentz force for a fundamental particle with charge q and velocity $\mathbf{v}$:

$$\mathbf{F} = q\mathbf{e} + \frac{q}{c}\mathbf{v} \times \mathbf{h} \tag{2.28}$$

Einstein called the four equations from Eq. (2.24) to Eq. (2.27), plus the Eq. (2.28), a complete set of Maxwell–Lorentz theory of electromagnetism.

It would be important to state the Maxwell's equations in the SI or MKS units, especially for the macroscopic problems in media. The unit transformation has been introduced in Tables 1.1 and 1.2 in Sect. 1.1. Actually we can follow some simple rules to transform the Maxwell's equations in cgs units from Eq. (2.18) to Eq. (2.21) into the MKS units (in cgs units, **E**, **D**, **H** and **B** have the same dimension; but in MKS units, both the ratio $[E/B]$ and $[H/D]$ have a dimension of speed c, the unit of **D** is C/m^2, and the unit of **H** is A/m):

$$\nabla \cdot \mathbf{D} = \rho_0, \tag{2.29}$$

$$\nabla \cdot \mathbf{B} = 0, \tag{2.30}$$

$$\nabla \times \mathbf{E} = -\frac{\partial \mathbf{B}}{\partial t}, \tag{2.31}$$

$$\nabla \times \mathbf{H} = \mathbf{j}_0 + \frac{\partial \mathbf{D}}{\partial t}, \tag{2.32}$$

where $(\rho_0, \mathbf{j}_0)$ are source of "free charge" in conductors. The Maxwell's equations Eqs. (2.29)–(2.32) also have to be solved self-consistently with the polarization equation of electric media in Eq. (1.4), the magnetization equation of magnetic media in Eq. (1.5), and the Ohm's law of conductors in Eq. (1.6).

2.2 Green's Function and Demagnetizing Matrix

The Green's function was brought up by George Green in 1824 to solve the electrostatic problem. If a point charge q is put at point $\mathbf{r}_0$ in a space with a conductor, the potential at another point $\mathbf{r}$ is contributed by the Coulomb potential from q and the potential from the induced charge on the surface of the conductor:

$$V(\mathbf{r}) = \frac{q}{|\mathbf{r} - \mathbf{r}_0|} + \iint \mathrm{d}^2\mathbf{r}' G(\mathbf{r}, \mathbf{r}')\sigma(\mathbf{r}') = \frac{q}{|\mathbf{r} - \mathbf{r}_0|} + \iint \mathrm{d}^2\mathbf{r}' \frac{\sigma(\mathbf{r}')}{|\mathbf{r} - \mathbf{r}'|}, \tag{2.33}$$

where the Green's function $G(\mathbf{r}, \mathbf{r}') = 1/|\mathbf{r} - \mathbf{r}'|$ is the solution in an infinite space of the Poisson equation with an unit point charge located at $\mathbf{r}'$:

$$\nabla^2 G(\mathbf{r}, \mathbf{r}') = -4\pi\delta^3(\mathbf{r} - \mathbf{r}'). \tag{2.34}$$

The Poisson equation developed by Siméon Poisson in 1811 is consistent with differential form of the Coulomb's law in Eq. (2.24) if we define the electric field $\mathbf{e} = -\nabla V$. The Green's function $G(\mathbf{r}, \mathbf{r}') = G(\mathbf{r}', \mathbf{r}) = 1/|\mathbf{r} - \mathbf{r}'|$ in an infinite space thus has the famous $1/r$ potential form, the same as the Coulomb potential.

The Green's function is important because it keeps the same form when the external charge q and the induced surface charge σ vary with time. When we try to solve the magnetic properties of a thin film or a device, although there is no intrinsic magnetic charge, the induced magnetic pole density ρ_{M} varies with the external field $\mathbf{H}_{\mathrm{ext}}$. This can be clarified by the differential form of the Gauss' law for magnetism in Eq. (2.19) and the magnetization equation in Eq. (1.5):

$$\nabla \cdot \mathbf{H} = 4\pi\rho_{\mathrm{M}} \ \ (\mathrm{cgs}); \qquad \rho_{\mathrm{M}} = -\nabla \cdot \mathbf{M}. \tag{2.35}$$

If the magnetization $\mathbf{M}$ is uniform in a grain or cell, the magnetic pole only exists on its surface. It is easy to prove by the Gauss law that the surface magnetic pole density is $\sigma_{\mathrm{M}} = \hat{n} \cdot \mathbf{M}$, where $\hat{n}$ is the unit vector normal to the surface.

In micromagnetics, the magnetic material is discretized into micromagnetic cells. Inside a cell, the moment $\mu = V_{\mathrm{c}}\mathbf{M}$ is assumed to rotate uniformly. Following the spirit of the Green's function, the demagnetizing matrix $\tilde{N}$ can be defined, where the magnetization $\mathbf{M}$ in a micromagnetic cell is the "source", and the magnetostatic interaction field or demagnetizing field $\mathbf{H}_{\mathrm{d}}$ is the "target":

$$\mathbf{H}_{\mathrm{d}}(\mathbf{r}) = \iiint \mathrm{d}^3\mathbf{r}' \left[-\nabla' \cdot \mathbf{M}(\mathbf{r}')\right] \frac{(\mathbf{r} - \mathbf{r}')}{|\mathbf{r} - \mathbf{r}'|^3} = -\tilde{N}(\mathbf{r}, \mathbf{0}) \cdot [\mathbf{4\pi M}], \tag{2.36}$$

$$\tilde{N}(\mathbf{r}, \mathbf{0}) = -\frac{1}{4\pi} \iiint_{V_{\mathrm{c}}} \mathrm{d}^3\mathbf{r}' \ \nabla'\nabla' \frac{1}{|\mathbf{r} - \mathbf{r}'|} = -\frac{1}{4\pi} \iint_{S} \mathrm{d}^2\mathbf{r}' \frac{(\mathbf{r} - \mathbf{r}')\hat{n}'}{|\mathbf{r} - \mathbf{r}'|^3}, \tag{2.37}$$

where the 3-D integral is made over the volume of the micromagnetic cell V_{c} (this is related to the fact that the magnetization $\mathbf{M}(\mathbf{r}') = \mathbf{M}$ is zero outside the cell), and the 2-D integral is made over the surface S of the cell. The $(\mathbf{r} - \mathbf{r}')\hat{n}'$ is a diad of the two vectors, and $\hat{n}'$ is the local normal at $\mathbf{r}'$ pointing outside the cell.

In micromagnetics, the demagnetizing matrix $\tilde{N}(\mathbf{r}_i, \mathbf{r}_j) = \tilde{N}(\mathbf{r}, \mathbf{0})$ only depends on the relative displacement $\mathbf{r} = \mathbf{r}_i - \mathbf{r}_j$ of the ith and jth micromagnetic cells, and it is independent of the magnetization of the cells. This characteristics is especially important when the problem is solved numerically, because $\tilde{N}$ can be computed in advance, stored and used repeatedly in calculation. Due to the intrinsic characteristics of the Green's function or the demagnetizing matrix, the trace is a conserved quantity when the target vector $\mathbf{r}$ is inside or outside of the micromagnetic cell:

$$\mathrm{Tr}\ \tilde{N}(\mathbf{r}, \mathbf{0}) = \sum_{\alpha} \mathbf{N}_{\alpha\alpha}(\mathbf{r}, \mathbf{0}) = \begin{cases} 1 & \mathbf{r} \text{ inside the cell} \\ 0 & \mathbf{r} \text{ outside the cell} \end{cases} \tag{2.38}$$

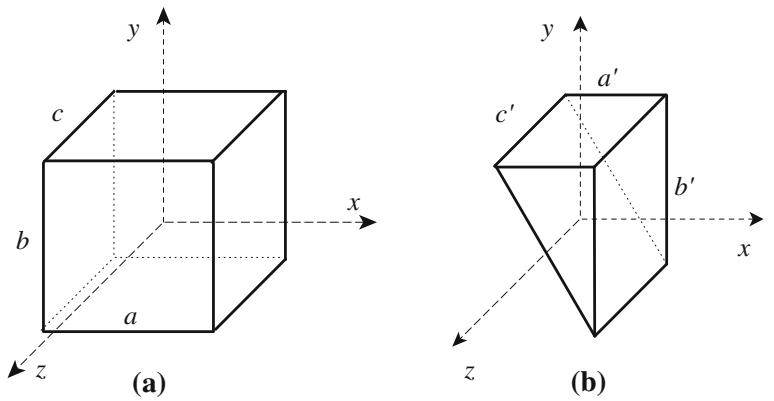

Fig. 2.3 Micromagnetic cells in a magnetic thin film. **a** Cuboid or cubic cell in the main body; **b** triangular prism cell at the edge; © [2009] IEEE. Reprinted, with permission, from Ref. [5]

Table 2.1 Demagnetizing matrix of a cuboic cell with uniform magnetization [7]

Cuboid cell size $a \times b \times c$	Integer variables $p = \pm 1, q = \pm 1, w = \pm 1$
Intermediate variable $\mathbf{R} = (R_1, R_2, R_3)$	$R_1 = \frac{a}{2} + px \quad R_2 = \frac{b}{2} + qy\ , \quad R_3 = \frac{c}{2} + wz$
Demagnetizing matrix element N_{11}	$\frac{1}{4\pi} \sum_p \sum_q \sum_w \tan^{-1}[R_2 R_3/(R_1 R)]$
Demagnetizing matrix element N_{22}	$\frac{1}{4\pi} \sum_p \sum_q \sum_w \tan^{-1}[R_3 R_1/(R_2 R)]$
Demagnetizing matrix element N_{33}	$\frac{1}{4\pi} \sum_p \sum_q \sum_w \tan^{-1}[R_1 R_2/(R_3 R)]$
Demagnetizing matrix element $N_{12} = N_{21}$	$\frac{1}{8\pi} \sum_p \sum_q \sum_w \ pq\ \ln[(R - R_3)/(R + R_3)]$
Demagnetizing matrix element $N_{13} = N_{31}$	$\frac{1}{8\pi} \sum_p \sum_q \sum_w \ pw\ \ln[(R - R_2)/(R + R_2)]$
Demagnetizing matrix element $N_{23} = N_{32}$	$\frac{1}{8\pi} \sum_p \sum_q \sum_w \ qw\ \ln[(R - R_1)/(R + R_1)]$

This is an useful property to check the correctness of the demagnetizing matrix.

Modern ferromagnetic devices are mostly made by thin films, as introduced in Sect. 1.3. To discretize an arbitrary-shaped device into micromagnetic cells, there are two basic classes for the geometry of cells: cuboid or cubic cell in the main body, and triangular prism cells at the edge, as seen in Fig. 2.3. The demagnetizing matrices of either cells can be calculated by Eq. (2.37), with a sum of contributions from all surfaces of the cell.

The demagnetizing matrix of a cuboid cell with a size $a \times b \times c$ can be integrated out directly [6]. Among the nine elements, there are only two independent types:

$$\tilde{N} = -\frac{1}{4\pi} \int_{-a/2}^{a/2} \mathrm{d}x' \int_{-b/2}^{b/2} \mathrm{d}y' \int_{-c/2}^{c/2} \mathrm{d}z' \ \nabla' \nabla' \frac{1}{|\mathbf{r} - \mathbf{r}'|} \tag{2.39}$$

$$N_{11} = \frac{1}{4\pi} \sum_{p=\pm 1} \iint \mathrm{d}y' \mathrm{d}z' \ \frac{a/2 + px}{\left[(a/2 + px)^2 + (y - y')^2 + (z - z')^2\right]^{3/2}} \tag{2.40}$$

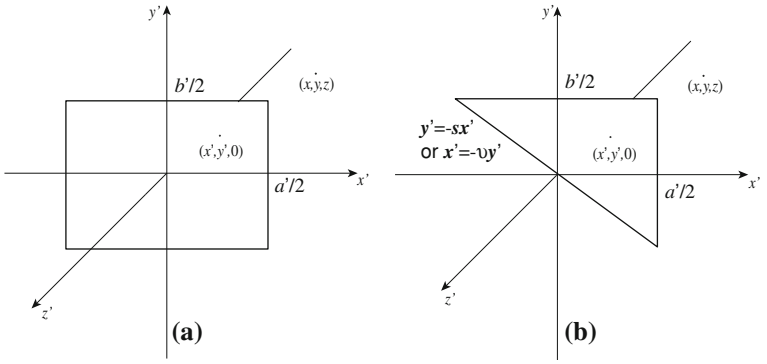

Fig. 2.4 Demagnetizing matrix contributed by poles on a 2-D surface. **a** Rectangle; **b** triangle; © [2009] IEEE. Reprinted, with permission, from Ref. [5]

$$N_{12} = -\frac{1}{4\pi} \sum_{p=\pm 1} \sum_{q=\pm 1} pq \int \frac{\mathrm{d}z'}{\left[(a/2+px)^2 + (b/2+qy)^2 + (z-z')^2\right]^{3/2}}, \tag{2.41}$$

where the sum integer variables $p, q = \pm 1$ come from the two integral limits. The nine elements in the demagnetizing matrix of a cuboic cell are listed in Table 2.1.

The demagnetizing matrix of a cuboid cell $\tilde{N}$ or a triangular prism cell $\tilde{N}^{(\mathrm{t})}$ (the center of cell locates at $\mathbf{0}$) in Fig. 2.3 can be calculated by summing over the contributions from the magnetic poles on the rectangle or triangle 2-D surfaces:

$$\tilde{N}(\mathbf{r}, \mathbf{0}) = \sum_{l=1}^{6} \tilde{R}_l \cdot \tilde{N}^{\mathrm{rec}} \left(\tilde{R}_l^{\mathrm{T}} \cdot (\mathbf{r} - \delta_l),\ \mathbf{0} \right) \cdot \tilde{R}_l^{\mathrm{T}} \tag{2.42}$$

$$\begin{aligned} \tilde{N}^{(\mathrm{t})}(\mathbf{r}, \mathbf{0}) = & \sum_{l=1}^{3} \tilde{R}_l \cdot \tilde{N}^{\mathrm{rec}} \left(\tilde{R}_l^{\mathrm{T}} \cdot (\mathbf{r} - \delta_l),\ \mathbf{0} \right) \cdot \tilde{R}_l^{\mathrm{T}} \\ & + \sum_{n=1}^{2} \tilde{R}_n \cdot \tilde{N}^{\mathrm{tri}} \left(\tilde{R}_n^{\mathrm{T}} \cdot (\mathbf{r} - \delta_n),\ \mathbf{0} \right) \cdot \tilde{R}_n^{\mathrm{T}} \end{aligned} \tag{2.43}$$

where $\tilde{N}^{\mathrm{rec}}$ or $\tilde{N}^{\mathrm{tri}}$ is the demagnetizing matrix of a rectangular or a right-angle triangular surface located in a fixed plane (say $z' = 0$), as seen in Fig. 2.4; $\tilde{R}$ is the 3-D rotational matrix between the real position of the respective surface in a micromagnetic cell ($x = \pm a/2$, $y = \pm b/2$, $z = \pm c/2$ for a cubic cell; or $x = a'/2$, $y = b'/2$, $y = -sx$, $z = \pm c'/2$ for a triangular prism cell) and the suppositional surface in the fixed $z' = 0$ plane; and δ is the displacement vector from the center of a cell to the face center of a square/rectangular surface, or from the center to the midpoint of the hypotenuse of a triangular surface, as labeled in Fig. 2.4.

Table 2.2 Demagnetizing matrix of a $a' \times b'$ rectangular surface at $z' = 0$ with uniform pole

Integer variables $q = \pm 1, w = \pm 1$, Intermediate variable $\mathbf{R} = (R_1, R_2, R_3)$
$R_1 = \frac{a'}{2} + qx,\ R_2 = \frac{b'}{2} + wy,\ R_3 = z, \quad R = \lvert\mathbf{R}\rvert = \sqrt{R_1^2 + R_2^2 + R_3^2}$
$N_{13}^{\rm rec} = -\frac{1}{4\pi}\sum_q \sum_w qw \ln(R - wR_2) = -\frac{1}{8\pi}\sum_q \sum_w q \ \ln[(R - R_2)/(R + R_2)]$
$N_{23}^{\rm rec} = -\frac{1}{4\pi}\sum_q \sum_w qw \ln(R - qR_1) = -\frac{1}{8\pi}\sum_q \sum_w w \ \ln[(R - R_1)/(R + R_1)]$
$N_{33}^{\rm rec} = -\frac{1}{4\pi}\sum_q \sum_w \arctan[R_1 R_2/(R_3 R)]$

Table 2.3 Demagnetizing matrix of a $a' \times b'$ right-angle triangular surface at $z' = 0$ with hypotenuse $y' = -sx'$ or $x' = -vy'$

$R_{\rm I} = \sqrt{\left(\frac{a'}{2} - x\right)^2 + R_2^2 + R_3^2},\ R_{\rm II} = \sqrt{R_1^2 + \left(\frac{b'}{2} - y\right)^2 + R_3^2}$
$c_1 = \frac{y - vx}{1+v^2},\ c_2^2 = \frac{r^2}{1+v^2} - c_1^2,\ P_2 = \frac{b'}{2} + wc_1,\ P = \sqrt{P_2^2 + c_2^2}$
$c_3 = \frac{x - sy}{1+s^2},\ c_4^2 = \frac{r^2}{1+s^2} - c_3^2,\ Q_1 = \frac{a'}{2} + qc_3,\ Q = \sqrt{Q_1^2 + c_4^2}$
$c_5 = y - \mathrm{i}z,\ \sqrt{(c_1 - c_5)^2 + c_2^2} = A\, e^{\mathrm{i}\theta'/2}$
$V_\pm = -wP_2 + \sqrt{P_2^2 + c_2^2} + c_1 - c_5 \pm A\, e^{\mathrm{i}\theta'/2} = \lvert V_\pm\rvert\, e^{\mathrm{i}\phi_\pm},$
$N_{13}^{\rm tri} = -\frac{1}{4\pi}\sum_w w \left\{\frac{1}{\sqrt{1+v^2}} \ln(P - wP_2) - \ln(R_{\rm I} - wR_2)\right\}$
$N_{23}^{\rm tri} = -\frac{1}{4\pi}\sum_q q \left\{\frac{1}{\sqrt{1+s^2}} \ln(Q - qQ_1) - \ln(R_{\rm II} - qR_1)\right\}$
$N_{33}^{\rm tri} = -\frac{1}{4\pi}\sum_w \arctan[(a'/2 - x)R_2/(R_3 R_{\rm I})]$
$\quad - \frac{1}{4\pi}\frac{zv}{\sqrt{1+v^2}}\sum_w \frac{w}{A}\left[+\ln\left\lvert\frac{V_+}{V_-}\right\rvert \cos\frac{\theta'}{2} + (\phi_+ - \phi_-)\sin\frac{\theta'}{2}\right]$
$\quad + \frac{1}{4\pi}\frac{x+vy}{\sqrt{1+v^2}}\sum_w \frac{w}{A}\left[-\ln\left\lvert\frac{V_+}{V_-}\right\rvert \sin\frac{\theta'}{2} + (\phi_+ - \phi_-)\cos\frac{\theta'}{2}\right]$

Definitions of $R_1,\ R_2,\ R_3,\ q$ and w are the same as in Table 2.2

The demagnetizing matrix $\tilde{N}^{\rm rec}(\mathbf{r}, \mathbf{0})$ or $\tilde{N}^{\rm tri}(\mathbf{r}, \mathbf{0})$, contributed by magnetic poles on a rectangular or a triangular surface, can be calculated by the 2-D integral in Eq. (2.37), where the target position locates at $\mathbf{r} = (x, y, z) = (r_1, r_2, r_3)$, as seen in Fig. 2.4. The integrations for nonzero elements of $\tilde{N}^{\rm rec}(\mathbf{r}, \mathbf{0})$ and $\tilde{N}^{\rm tri}(\mathbf{r}, \mathbf{0})$ [5]

$$N_{\alpha 3}^{\rm rec}(\mathbf{r}, \mathbf{0}) = -\frac{1}{4\pi}\int_{-a'/2}^{a'/2} \mathrm{d}r_1' \int_{-b'/2}^{b'/2} \mathrm{d}r_2' \frac{r_\alpha - r_\alpha'}{\left[(r_1 - r_1')^2 + (r_2 - r_2')^2 + r_3^2\right]^{3/2}} \tag{2.44}$$

$$N_{\alpha 3}^{\rm tri}(\mathbf{r}, \mathbf{0}) = -\frac{1}{4\pi}\int_{-b'/2}^{b'/2} \mathrm{d}y' \int_{-vy'}^{a'/2} \mathrm{d}x' \frac{r_\alpha - r_\alpha'}{\left[(r_1 - r_1')^2 + (r_2 - r_2')^2 + r_3^2\right]^{3/2}} \tag{2.45}$$

$$= -\frac{1}{4\pi}\int_{-a'/2}^{a'/2} \mathrm{d}x' \int_{-sx'}^{b'/2} \mathrm{d}y' \frac{r_\alpha - r_\alpha'}{\left[(r_1 - r_1')^2 + (r_2 - r_2')^2 + r_3^2\right]^{3/2}} \tag{2.46}$$

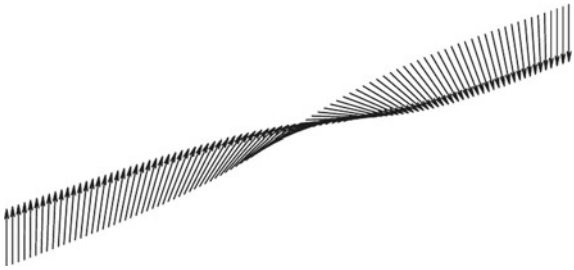

Fig. 2.5 Bloch wall between two domains: $m_z = \tanh(x/a)$ where wall width $a = \sqrt{A^*/K_1}$

are given in the Appendix. The analytical expressions of $N_{\alpha 3}^{\text{rec}}(\mathbf{r}, \mathbf{0})$ and $N_{\alpha 3}^{\text{tri}}(\mathbf{r}, \mathbf{0})$ ($\alpha = 1, 2, 3$) are given in Tables 2.2 and 2.3, respectively.

Using the results of the surface demagnetizing matrices given in Tables 2.2 and 2.3, together with the definitions of the demagnetizing matrices of a cubic/cuboid cell and a triangular prism cell in Eqs. (2.42) and (2.43) respectively, the magnetostatic interaction field can be calculated for any micromagnetic cell in a ferromagnetic thin film or device with a flat structure. In more complicated device with 3-D structures, the surface of any edge micromagnetic cell can still be divided into rectangles and right-angle triangles, thus the respective demagnetizing matrix can also be found analytically using the similar methods as in Eq. (2.43).

2.3 Landau–Lifshitz Equations

In 1935, Landau and Lifshitz brought up a free energy expression for ferromagnetic materials [8]; furthermore, a dynamic equation of spins, called LL equation later, was given to analyze the motion of Bloch domain wall in Fig. 2.5. These works built the fundamentals of applied magnetic theory.

As discussed in Sect. 1.2, in 1907, Pierre-Ernest Weiss brought up the concept of a huge spontaneous magnetic field to explain the alignment of the elementary magnets (atomic spins) in a ferromagnetic material even without an external field. The spontaneous magnetization is related to the crystal structure, which orients to the easy axis. A single crystal contains a large amount of "domains", and the size of a Weiss domain is assumed to be 10–100 nm.

The modern magnetization-curve theory was founded by Akulov and Becker. In 1929, Akulov derived the anisotropy energy for Fe and Ni [9]; in 1930, Becker introduced a rigid rotational model to find the loops of a particle [10]. In 1932, Bloch worked out a structure of the boundary wall between two Weiss domains [11], now known as the "Bloch wall", although its common expression $m_z = \tanh(x/a)$ was given by Landau [8]. The concept of "Micromagnetics" was brought up by Brown in 1958. The rise of computational science in 1940s made it possible to solve the LL equations numerically, which led to the micromagnetic theory today for ferromagnetic materials.

2.3.1 Free Energy and Effective Field

Landau was a master of phenomenological theory in condensed matter physics. In the free energy $\mathscr{F}$ of a ferromagnet, the magnetization vector $\mathbf{M} = M_s\hat{m}$ takes the role of "position vector" $\mathbf{r}$ as in mechanics, the Zeeman energy $\mathscr{E}_{\text{ext}}$ due to the external magnetic field, the anisotropy energy $\mathscr{E}_{\text{a}}$ describing the Weiss spontaneous magnetization, the exchange energy $\mathscr{E}_{\text{ex}}$ of Heiseberg model, the magnetostatic interaction energy $\mathscr{E}_{\text{m}}$, and the magneto-elastic energy $\mathscr{E}_{\sigma}$ are included [1]:

$$\mathscr{F}(\{\hat{m}\}) = \mathscr{F}_0 + \mathscr{E}_{\text{ext}} + \mathscr{E}_{\text{a}} + \mathscr{E}_{\text{ex}} + \mathscr{E}_{\text{m}} + \mathscr{E}_{\sigma}, \tag{2.47}$$

$$\mathscr{E}_{\text{ext}} = -\iiint \mathrm{d}^3\mathbf{r}\ \ M_s\hat{m}(\mathbf{r}) \cdot \mathbf{H}_{\text{ext}}(\mathbf{r}), \tag{2.48}$$

$$\mathscr{E}_{\text{a}} = \iiint \mathrm{d}^3\mathbf{r}\ \ \left(K^{(1)}_{ij} m_i m_j + K^{(2)}_{ijkl} m_i m_j m_k m_l + \mathrm{o}(m^6)\right), \tag{2.49}$$

$$\mathscr{E}_{\text{ex}} = \frac{1}{2}\iiint \mathrm{d}^3\mathbf{r}\ \ (2A^*_{ij})(\partial_i m_l)(\partial_j m_l), \tag{2.50}$$

$$\begin{aligned}\mathscr{E}_{\text{m}} &= -\frac{1}{2}\iiint \mathrm{d}^3\mathbf{r}\ \ M_s\hat{m}(\mathbf{r}) \cdot \mathbf{H}_{\text{d}}(\mathbf{r}) \\ &= \frac{1}{2}(4\pi M_s^2) \sum_{\mathbf{r}} V_{\mathbf{r}} \sum_{\mathbf{r}'} \hat{m}(\mathbf{r}) \cdot \tilde{N}(\mathbf{r}, \mathbf{r}') \cdot \hat{m}(\mathbf{r}'),\end{aligned} \tag{2.51}$$

$$\mathscr{E}_{\sigma} = -\iiint \mathrm{d}^3\mathbf{r}\, a_{ijkl}\, \sigma_{ij}\, m_k m_l, \tag{2.52}$$

where Einstein notation is used to sum all the dummy indices from 1 to 3. In Eq. (2.49), the first two orders of crystalline anisotropy energy are included, which are both important in crystals with different symmetries. In Eq. (2.50), the exchange constant $2A^*$ is the parameter α in Landau and Lifshitz's original paper [8]; $2A^*$ but not A^* is utilized because in this way A^* has a direct relationship with the exchange energy J_{e} in the Heisenberg model discussed in Sect. 1.2: $A^* = J_{\text{e}}/R$ where R is the nearest neighbor (NN) atomic distance. In Eq. (2.51), the demagnetizing field $\mathbf{H}_{\text{d}}$ is similar to the one given in Eq. (2.36), except that the $\mathbf{H}_{\text{d}}$ here is contributed by all micromagnetic cells $\mathbf{r}'$ in the medium; in the second line of this equation, a sum but not an integral over the volume $V_{\mathbf{r}}$ is utilized, because the concept of "demagnetizing matrix" $\tilde{N}$ in Eq. (2.37) has to be defined in a finite-size volume $V_{\mathbf{r}'}$. In Eq. (2.52), σ_{ij} is the stress matrix, and the fourth-order tensor parameter a_{ijkl} links the magnetic property and the mechanical property in a crystal; this term can also be used at the interface of thin films, where the stress σ_{ij} is nonzero only in several atomic planes, but this will be very important to explain the thin film properties.

The free energy of crystalline anisotropy in Eq. (2.49) needs to be further discussed for different crystal symmetries. In general, we can prove the characteristics of the parameter matrix $K^{(1)}_{ij}$ by the rotational invariant under all rotational matrices $\tilde{R}$ of a certain symmetry:

$$\tilde{K}^{(1)} = \tilde{R} \cdot \tilde{K}^{(1)} \cdot \tilde{R}^{\text{T}} \tag{2.53}$$

For cubic crystals such as iron and nickel, if we use two successive $\tilde{R}$ of C_4 operation, the off-diagonal matrix elements $K_{ij}^{(1)}$ $(i \neq j)$ can be proved to be zero; then by using $\tilde{R}$ of C_3 operation, we can proved that $K_{11}^{(1)} = K_{22}^{(1)} = K_{33}^{(1)}$. However, under the constraint of $\hat{m}^2 = 1$, the term of $K_{ij}^{(1)}$ is trivial. The next order parameter $K_{ijkl}^{(2)}$ can be treated as the diad of two matrices. Still, by two successive $\tilde{R}$ of C_4 operation and another $\tilde{R}$ of C_3 operation, we can prove that there are only two kinds of nonzero independent parameters in this term: $K_a = K_{iijj}^{(2)} = K_{ijij}^{(2)} = K_{ijji}^{(2)}$ and $K_b = K_{iiii}^{(2)}$, and the cubic crystalline anisotropy energy is in the form [9]:

$$\mathscr{E}_{\mathrm{a}}^{(\mathrm{c})} = \iiint \mathrm{d}^3\mathbf{r} \left\{ 2K_1[(\hat{m}\cdot\hat{k}_1)^2(\hat{m}\cdot\hat{k}_2)^2 + (\hat{m}\cdot\hat{k}_2)^2(\hat{m}\cdot\hat{k}_3)^2 + (\hat{m}\cdot\hat{k}_3)^2(\hat{m}\cdot\hat{k}_1)^2] + K_2(\hat{m}\cdot\hat{k}_1)^2(\hat{m}\cdot\hat{k}_2)^2(\hat{m}\cdot\hat{k}_3)^2 \right\} \quad (2.54)$$

The $\hat{k}_1, \hat{k}_2, \hat{k}_3$ are cubic axes; $K_1 = 3K_a - K_b$ is positive for Fe and negative for Ni.

For a hexagonal crystal such as cobalt, it is easy to prove that, for $K_{ij}^{(1)}$ matrix, there are only two nonzero independent elements $K_{11}^{(1)} = K_{22}^{(1)}$ and $K_{33}^{(1)}$ if we use $\tilde{R}$ of C_6 group with $\theta = \pi$ and $\theta = \pi/3$. Furthermore, by using the constraint $m_x^2 + m_y^2 + m_z^2 = 1$, there is only one independent parameter $K_1 = K_{11}^{(1)} - K_{33}^{(1)}$ left. Then, the hexagonal anisotropy energy must be in the form [1]:

$$\mathscr{E}_{\mathrm{a}}^{(\mathrm{h})} = \iiint \mathrm{d}^3\mathbf{r} \left\{ K_1[\hat{m}\times\hat{k}_c]^2 + K_2[\hat{m}\times\hat{k}_c]^4 \right\} \quad (2.55)$$

where K_2 is the second-order term which can be proved by the symmetry of $K_{ijkl}^{(2)}$.

The magnetic recording media such as CoPt and FePt have a tetragonal symmetry of $L1_0$ phase. The fourfold symmetry axis is the c-axis or z-axis, by using two successive $\tilde{R}$ of C_4 operation around c-axis, we can prove that $K_{u1} = K_{11}^{(1)} = K_{22}^{(1)}$. Both the hexagonal and tetragonal anisotropy are called "uniaxial anisotropy", because the first term in their crystalline anisotropy is $K_{u1}\sin^2\theta$ or $-K_{u1}\cos^2\theta$ around the c-axis. In the term of $K_{ijkl}^{(2)}$, there are also two classes of independent parameters. Then the tetragonal crystalline anisotropy energy is in the form [1]:

$$\mathscr{E}_{\mathrm{a}}^{(\mathrm{t})} = \iiint \mathrm{d}^3\mathbf{r} \left\{ -K_{u1}(\hat{m}\cdot\hat{k}_c)^2 - K_{u2}\left[1-(\hat{m}\cdot\hat{k}_c)^2\right]^2 - K_{\mathrm{c}}(\hat{m}\cdot\hat{k}_a)^2(\hat{m}\cdot\hat{k}_b)^2 \right\} \quad (2.56)$$

where $\hat{k}_a$, $\hat{k}_b$, $\hat{k}_c$ are the crystal axes for a tetragonal conventional unit cell. The details of the second-order parameters K_{u2} and K_{c} depend on the degree of order of the alloy, and usually K_{c} is more important and harder to control in experiment.

Table 2.4 Anisotropy constants and exchange field constants $H_e = 2A^*/(M_s D^2)$

FM Crystals	Fe	Co	Ni
M_s(emu/g)	221.71 ± 0.08	162.55	58.57 ± 0.03
M_s(emu/cm^3)	1742.6	1446.7	521.3
K_1(erg/cm^3)	4.81×10^5	4.12×10^6	-5.5×10^4
K_2(erg/cm^3)	1.2×10^3	1.43×10^6	-2.5×10^4
Easy axis	$\hat{k}_1$, $\hat{k}_2$, $\hat{k}_3$	$\hat{k}_c$	$\hat{k}_1 + \hat{k}_2 + \hat{k}_3$
$H_k = 2K_1/M_s$(Oe)	552	5,696	−221
H_e(Oe) with $D = 10$ nm	1,148	1,382	3,827
H_e(Oe) with $D = 2$ nm	28,700	34,550	95,675

D is the micromagnetic cell size, A^* is assumed to be on the order of 1×10^{-6} erg/cm, for Fe, Co and Ni

The micromagnetics is not an atomic or electronic scale theory; therefore the basic magnetic parameters such as M_s, K_1 and A^* have to be treated as the input of the model. Actually in practical alloy or composite magnetic materials, these basic parameters can not be provided by either accurate theoretical calculation or direct experimental measurement. The experiment-simulation cycles have to be done to fit these parameters M_s, K_1 and A^*. In Table 1.3, the structure and crystalline characteristics of ferromagnetic crystals have been given, here in Table 2.4, the anisotropy energy constant and exchange field constant of Fe, Co, Ni are given respectively.

In a magnetic material, the effective magnetic field $\mathbf{H}_{\text{eff}}$ felt by a micromagnetic cell at $\mathbf{r}$ can be found by the variation $\mathbf{H}_{\text{eff}}(\mathbf{r}) = -\delta\mathscr{F}/\delta(M_s\hat{m}(\mathbf{r}))$ in the continuum integration form in Eqs. (2.49)–(2.52) or by the derivation $\mathbf{H}_{\text{eff}} = -\partial\mathscr{F}/\partial(V_{\mathbf{r}} M_s \hat{m}(\mathbf{r}))$ in the discretized summation form over $\mathbf{r}$ in Eq. (2.51) (cgs units):

$$\mathbf{H}_{\text{eff}}(\mathbf{r}) = \mathbf{H}_{\text{ext}}(\mathbf{r}) + \mathbf{H}_a(\mathbf{r}) + \mathbf{H}_{\text{ex}}(\mathbf{r}) + \mathbf{H}_m(\mathbf{r}) + \mathbf{H}_\sigma(\mathbf{r}). \tag{2.57}$$

$$\mathbf{H}_a(\mathbf{r}) = H_k \left(\hat{e}_i \, K_{ij}^{(1)} m_j + \hat{e}_i \, 2K_{ijkl}^{(2)} m_j m_k m_l + o(m^5) \right) / K_1, \tag{2.58}$$

$$\mathbf{H}_{\text{ex}}(\mathbf{r}) = (2\hat{e}_l/M_s) \, A_{ij}^* \partial_i \partial_j m_l \simeq H_e \sum_{\mathbf{r}'}^{\text{NN}} \left(\hat{m}(\mathbf{r}') - \hat{m}(\mathbf{r}) \right), \tag{2.59}$$

$$\mathbf{H}_m(\mathbf{r}) = -(4\pi M_s) \sum_{\mathbf{r}'} \tilde{N}(\mathbf{r}, \mathbf{r}') \cdot \hat{m}(\mathbf{r}'), \tag{2.60}$$

$$\mathbf{H}_\sigma(\mathbf{r}) \simeq H_{\text{me}} \, (\hat{m}(\mathbf{r}) \cdot \hat{e}_x)\hat{e}_x + H'_{\text{me}} \left[(\hat{m}(\mathbf{r}) \cdot \hat{e}_y)\hat{e}_x + (\hat{m}(\mathbf{r}) \cdot \hat{e}_x)\hat{e}_y \right], \tag{2.61}$$

where Einstein notation is still used in three of previous equations. In Eq. (2.58), the anisotropy field constant $H_k = 2K_1/M_s$, and the relationship among K_1, $K_{ij}^{(1)}$ and $K_{ijkl}^{(2)}$ has been discussed in crystals with different symmetries. For cubic symmetry, the term of $K_{ij}^{(1)}$ will not appear, since it is a trivial or constant term.

Furthermore, if a clearer vector form of anisotropy field is to be used, the derivative $\mathbf{H}_\mathrm{a} = -\partial \mathscr{E}_\mathrm{a}/\partial(V_\mathbf{r} M_\mathrm{s} \hat{m}(\mathbf{r}))$ can be taken directly for Eqs. (2.55)–(2.56).

In Eq. (2.59), the exchange field constant is $H_\mathrm{e} = 2A^*/(M_\mathrm{s} D^2)$ where D is the micromagnetic cell size. In the original form of Landau and Lifshitz [1], the exchange constant A^*_{jl} also depends on the crystal symmetry. Inside a micromagnetic cell, the magnetic moment is assumed to rotate uniformly. With two neighbor cells at a distance of D, which is usually larger than 1 nm, at least one order larger than atomic distance R, the exchange field constant $H_\mathrm{e} = 2J_\mathrm{e}/(M_\mathrm{s} D^2 R)$ is much smaller than the Weiss field $H_\mathrm{E} \simeq z J_\mathrm{e}/(M_\mathrm{s} R^3) \sim 10^7$ Oe among neighbor atoms, where z is the number of NN atomic spins. Therefore, we can make an approximation $A*_{ij} \simeq A^* \delta_{ij}$ and omit the crystal asymmetry in Eq. (2.59), where the sum over $\mathbf{r}'$ is only taken over the NN cells of the cell at $\mathbf{r}$.

In Eq. (2.60), the sum over $\mathbf{r}'$ is taken over micromagnetic cells discretized at a distance D in any dimension, similar to Eq. (2.59). When $\mathbf{r}' = \mathbf{r}$, the term in the sum $-B_\mathrm{s} \tilde{N}(\mathbf{r}, \mathbf{r}) \cdot \hat{m}(\mathbf{r})$ is called the shape anisotropy field, whose expression is actually more complicated due to the constraint $\hat{m}^2 = 1$; however we will prove that it is equivalent to the term here when used in LL equations. As discussed in Sect. 2.2, sometimes the micromagnetic is not a simple cube, but a polyhedron, then the demagnetizing matrix $\tilde{N}$ should be calculated following a formula similar to Eq. (2.43) by summing over the contributions of demagnetizing matrices of a rectangle surface and a triangle surface in Tables 2.2 and 2.3.

In Eq. (2.61), the magneto-elastic field due to interfacial stress is largely simplified. The H_me is the magneto-elastic field constant along an in-plane direction $\hat{e}_x$, and H'_me is related to the $m_x m_y$ energy term, if the thin film is in x–y plane.

2.3.2 LL Equation and LLG Equation

In 1935, Landau worked in the Haerkof University and the Physico-Technical Institute, Academy of Science, in Ukraine, USSR. Landau and his student Lifshitz brought up the famous LL equation in their theory of magnetic domain and domain wall resonance. The first term in LL equation can be derived from the Heisenberg equation of spin, which is related to the energy conservation of magnetic free energy. The second term in LL equation was said to be originated from the relativistic interaction between the magnetic moment and the crystal in the original paper [8]; nowadays this nonlinear second term is believed to be caused by the dissipative process, which is complicated and hard to be explained accurately, just similar to the frictional force (Fig. 2.6).

As discussed in Sect. 1.2, the atomic magnetic moment $\mu_\mathrm{a} = -g\mu_\mathrm{B}\mathbf{S}$, where g is the g-factor, μ_B is the Bohr magnet, $\mathbf{S}$ is the atomic spin. If we omit energy dissipation, the eigenvalue of Hamiltonian $\mathscr{H} = -\mu_\mathrm{a} \cdot \mathbf{H}$, is conserved; then we can use the Heisenberg's equations to describe the motion of spin $\mathbf{S} = \hat{e}_i \, S_i$:

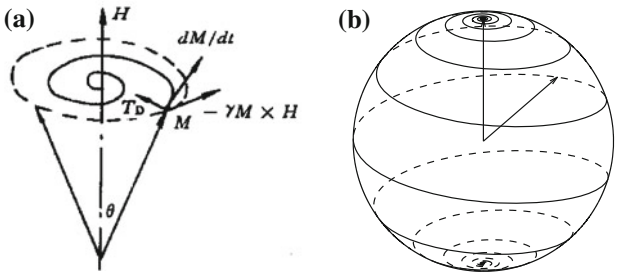

Fig. 2.6 Landau–Lifshitz equation. **a** Directions of precession term and damping term; **b** switching process of a magnetic moment or a spin from $+z$ to $-z$ direction by an external field

$$\frac{\mathrm{d}S_i}{\mathrm{d}t} = \frac{1}{\mathrm{i}\hbar}[S_i,\ \mathscr{H}] = \frac{g\mu_\mathrm{B}}{\mathrm{i}\hbar}[S_i, S_j]\, H_j = \frac{g\mu_\mathrm{B}}{\hbar}\varepsilon_{ijk} S_k H_j \tag{2.62}$$

where the commutator of the spin is $[S_i, S_j] = \mathrm{i}\,\varepsilon_{ijk} S_k$. In a ferromagnetic material, near the 0 K, the atomic moment in a cell can be written as: $\mathbf{M} = n\mu = -ng\mu_\mathrm{B}\mathbf{S}$, where n is the atomic density. Based on Eq. (2.62), if the energy is conserved, the equation of motion of magnetic moment is in the form:

$$\frac{\mathrm{d}\mathbf{M}}{\mathrm{d}t} = -ng\mu_\mathrm{B}\frac{\mathrm{d}\mathbf{S}}{\mathrm{d}t} = -g\frac{\mathrm{e}}{2mc}(\mathbf{M}\times\mathbf{H}) = -\gamma_0(\mathbf{M}\times\mathbf{H}) \tag{2.63}$$

where the constant $\gamma_0 = ge/2mc$ is the gyromagnetic ratio for an atomic spin. For the ferromagnetic alloys of Fe, Co, Ni transition metal elements, due to the quenching of orbital angular momentum of d-electrons, the g-factor of atomic spin usually is just the $g_0 = 2$ of an electron. Therefore the gyromagnetic ratio in the LL equation usually takes the value $\gamma_0 = e/mc = 1.75882 \times 10^7\,\mathrm{Oe}^{-1}\,\mathrm{s}^{-1}$.

When the dissipation of magnetic free energy is included, the atomic spins have a non-equilibrium statistics, and its motion becomes nonlinear. Based on the Hamiltonian $\mathscr{H} = -\mu_\mathrm{a}\cdot\mathbf{H}$, the dissipation of magnetic energy means the moment $\mathbf{M}$ will rotate to the direction of local magnetic field $\mathbf{H}$, which equals the effective magnetic field $\mathbf{H}_\mathrm{eff}$. Therefore Landau and Lifshitz added a damping term in the equation of motion of spin, which results in the famous LL equation:

$$\frac{\mathrm{d}\mathbf{M}}{\mathrm{d}t} = -\gamma(\mathbf{M}\times\mathbf{H}_\mathrm{eff}) - \gamma\frac{\alpha}{M}\mathbf{M}\times(\mathbf{M}\times\mathbf{H}_\mathrm{eff}) \tag{2.64}$$

where the dimensionless constant α is called the Landau damping constant, which reveals the dissipation speed in the ferromagnetic material. Similar to the frictional coefficient, the damping constant α is also phenomenological. Usually in Fe, Co, Ni metals or alloys, α is less than 0.1, sometimes even below 0.01. However, in ferromagnetic oxides or ferrites, the dissipation process is much slower, thus α can be one or two orders lower than the value in ferromagnetic metals.

In micromagnetics, the equation of motion for magnetic moments is always called the LLG equation, because an American scientist Thomas Gilbert explained the damping term of LL equation by the dissipative Lagrange equation with a Rayleigh's dissipation function in 1955 [12]:

$$\frac{\mathrm{d}}{\mathrm{d}t}\frac{\delta \mathscr{L}[\mathbf{M},\dot{\mathbf{M}}]}{\delta \dot{\mathbf{M}}} - \frac{\delta \mathscr{L}[\mathbf{M},\dot{\mathbf{M}}]}{\delta \mathbf{M}} + \frac{\delta \mathscr{R}[\dot{\mathbf{M}}]}{\delta \dot{\mathbf{M}}} = 0 \tag{2.65}$$

where Gilbert assumed that the Lagrange equation itself will result in the Eq. (2.63) of motion for the magnetic moment under the constraint of energy conservation. In the Lagrange $\mathscr{L}[\mathbf{M},\dot{\mathbf{M}}] = \mathscr{T} - \mathscr{U}$, the role of magnetization $\mathbf{M}$ is the same as the position $\mathbf{r}$ in $\mathscr{L}[\mathbf{r},\dot{\mathbf{r}}]$ of classical mechanics. The Rayleigh dissipation functional is also constructed analogous to that of the frictional force in mechanics:

$$\mathscr{R}[\dot{\mathbf{r}}] = \frac{\eta}{2}\iiint \mathrm{d}^3\mathbf{r}\,\dot{\mathbf{r}}^2(\mathbf{r},t) \quad \Rightarrow \quad \mathscr{R}[\dot{\mathbf{M}}] = \frac{\eta}{2}\iiint \mathrm{d}^3\mathbf{r}\,\dot{\mathbf{M}}^2(\mathbf{r},t) \tag{2.66}$$

Then the LLG equation can be obtained by inserting the Rayleigh dissipation functional into Eq. (2.65), where the effective field appears as $\delta\mathscr{U}/\delta\mathbf{M} = -\mathbf{H}_{\mathrm{eff}}$:

$$\begin{aligned}&\frac{\mathrm{d}}{\mathrm{d}t}\frac{\delta \mathscr{T}[\mathbf{M},\dot{\mathbf{M}}]}{\delta \dot{\mathbf{M}}} - \frac{\delta \mathscr{T}[\mathbf{M},\dot{\mathbf{M}}]}{\delta \mathbf{M}} + \left(-\mathbf{H}_{\mathrm{eff}} + \eta\dot{\mathbf{M}}\right) = 0 \Rightarrow \\ &\frac{\partial \mathbf{M}}{\partial t} = -\gamma_0\mathbf{M}\times\left(\mathbf{H}_{\mathrm{eff}} - \eta\dot{\mathbf{M}}\right) = -\gamma_0\mathbf{M}\times\mathbf{H}_{\mathrm{eff}} + \frac{\alpha}{M}\mathbf{M}\times\frac{\partial \mathbf{M}}{\partial t}\end{aligned} \tag{2.67}$$

where the damping $\alpha = \gamma_0\eta M$. The explicit expression for the kinetic energy $\mathscr{T}[\mathbf{M},\dot{\mathbf{M}}]$ of a rotating body is quite complicated, thus the derivation in Eq. (2.67) from the first line to the second line is obtained by the argument that this equation must be equivalent to Eq. (2.63) when the "friction coefficient" $\eta = 0$ [12].

The LLG equation and LL equation is totally equivalent to one another, except that the gyromagnetic ratio γ in the two equations has a small difference related to the damping. If we insert the right-hand side of the LLG equation in Eq. (2.67) into the last term $\partial\mathbf{M}/\partial t$, it is easy to prove that:

$$(1+\alpha^2)\frac{\partial \mathbf{M}}{\partial t} = -\gamma_0\mathbf{M}\times\mathbf{H}_{\mathrm{eff}} - \gamma_0\frac{\alpha}{M}\mathbf{M}\times(\mathbf{M}\times\mathbf{H}_{\mathrm{eff}}) \tag{2.68}$$

Comparing this Eq. (2.68) with the LL Eq. (2.64), it is clear that:

$$\gamma = \gamma_0/(1+\alpha^2) \tag{2.69}$$

Therefore the gyromagnetic ratio γ in the LL equation should be smaller than the gyromagnetic ratio γ_0 in the LLG equation, by a small factor related to the damping coefficient α.

2.3.3 History of Micromagnetics

The phrase "micromagnetics" was brought up by Brown in 1958, now it becomes the mainstream theory for computational applied magnetism. In Brown's book *Micromagnetics* [13], he summarized the "magnetization curve theory" and "domain theory" before 1960s, which are the main parts of today's micromagnetics. Furthermore, he studied the LL equation with the linear approximation or by the nonlinear calculation of static and dynamic problems.

The predecessor of micromagnetics was the magnetization-curve theory. The earliest theory of "induced magnetization" was given by W. E. Weber in 1852. The modern magnetization-curve theory was founded by Akulov and Becker. In 1929, Akulov derived the anisotropy energy for Fe and Ni with the cubic crystalline symmetry [9], as given in Eq. (2.54). To explain the magnetization curve of single crystals, as shown in Fig. 2.7a–c, a rigid rotation approximation can be used to explain the curve by minimizing the total energy $\mathscr{E}_\mathrm{a} - \mathbf{H} \cdot \mathbf{M}$.

In Table 2.5, the expression of the anisotropy energy $\mathscr{E}_\mathrm{a}$ and the derived magnetization curve, i.e. the $\bar{M}-H$ relationship, are listed in the hard axes for Fe, Co and Ni single crystal, respectively. It should be noted that the expressions of $\mathscr{E}_\mathrm{a}$ for Fe and Ni are equivalent, except a constant, because both Fe and Ni have the cubic symmetry. M–H curves listed in Table 2.5 are also plotted in Fig. 2.7d–f.

If we compare the measured and the calculated magnetization curves under the rigid rotation approximation, several conclusions can be made. First, the remanence of M–H curves along hard axes can be estimated quite well. Secondly, the saturation field is on the order of the anisotropy field constant $H_\mathrm{k} = 2K_1/M_\mathrm{s}$; however, it can be seen in Fig. 2.7 and Table 2.5 that, in Fe, Co, Ni, the saturation field is about H_k, $0.15H_\mathrm{k}$ and $0.65H_\mathrm{k}$ respectively; therefore only the sample of Fe in Kaya's experiment [14] was near a single crystal. Most importantly, the M–H curve in the easy axis can not be explained by the rigid rotation model.

Thus Bloch's domain wall theory brought up during 1930–1931 was natural and necessary to explain these non-uniform rotation phenomena. A Bloch wall has a structure with zero pole density $\rho_\mathrm{M} = -\nabla \cdot \mathbf{M}$; Therefore the magnetostatic interaction energy can be neglected in the free energy. Actually this was an approximation used in most of the early magnetization-curve theory and domain theory [8].

The M–H loop of single-domain particle was an important topic too in the magnetic theory. In 1930, Becker introduced the rigid rotational model, in conjunction with the concept of "internal stress", to explain the loops of an element in a magnetic material. The total free energy of this element was [10]:

$$U = U_\mathrm{dip} - \mathbf{H} \cdot \mathbf{J} = -2SAJ^2 \cos(2(\theta - \varepsilon)) - HJ\cos\theta, \tag{2.70}$$

where S is a coefficient, A is the internal stress, J is the magnetization, θ is the angle between $\mathbf{J}$ and $\mathbf{H}$, and ε is the angle between $\mathbf{H}$ and the original position $\mathbf{B}$ of $\mathbf{J}$ when $\mathbf{H} = 0$ (along the stress anisotropy). Becker derived the M–H loop at different angle ε, where horizontal axis is H/H_σ with $H_\sigma = 4SAJ$, as seen in Fig. 2.8.

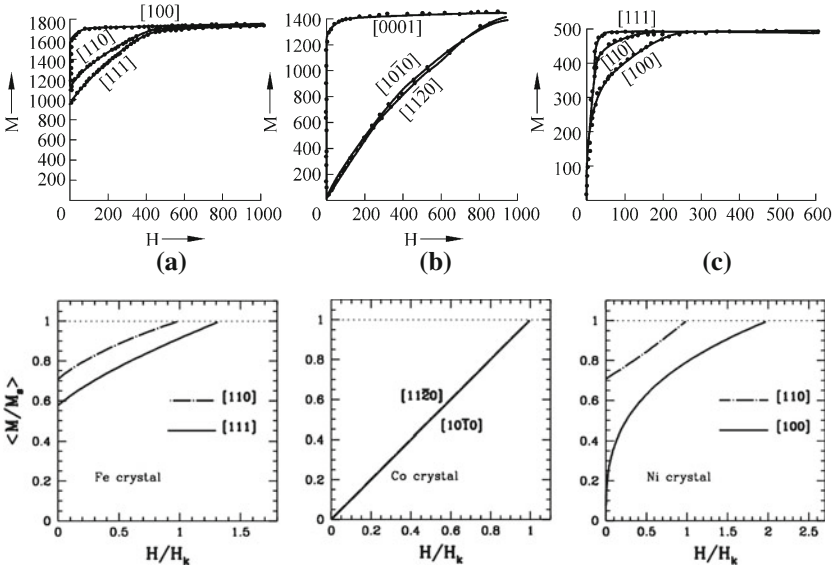

Fig. 2.7 **a–c** Measured M–H loops of Fe, Co, Ni [14]; **d–f** calculated M–H curves in the hard axes of single crystal Fe, Co, Ni under the rigid rotation approximation

Table 2.5 Magnetization curve $\bar{M} = \mathbf{M} \cdot \mathbf{H}/(M_s H)$ of Fe, Co, Ni by the rigid rotation model

Crystal	Fe	Co	Ni
$\mathscr{E}_a$	$2K_1(m_1^2m_2^2 + m_2^2m_3^2 + m_3^2m_1^2)$	$K_1(m_1^2 + m_2^2)$	$-K_1(m_1^4 + m_2^4 + m_3^4)$
M_s	1742.6 emu/cm^3	1446.7 emu/cm^3	521.3 emu/cm^3
H_k	552 Oe	5696 Oe	−221 Oe
M–H 1	$H_{[110]}/H_k = \bar{M}(2\bar{M}^2 - 1)$	$H_{[11\bar{2}0]}/H_k = \bar{M}$	$H_{[110]}/H_k = (2\bar{M}^2 - 1)/\bar{M}$
M–H 2	$H_{[111]}/H_k = \frac{(3\bar{M}^3 - \bar{M})}{1+(3\bar{M}^2-1)/4}$	$H_{[10\bar{1}0]}/H_k = \bar{M}$	$H_{[100]}/H_k = 2\bar{M}^3$

The famous Stoner–Wohlfarth model [15, 16] of a single-domain particle's M–H loop was mathematically equivalent to Becker's work. However, the physical explanation of the effective anisotropy energy of the single particle or element was different. In the first 50 years of magnetic recording, the magnetic media were granular or particulate media, which were composed of elongated particles such as γ-Fe_2O_3. The γ-Fe_2O_3 has a complicated cubic structure, and its crystalline anisotropy is small. In a recording medium, γ-Fe_2O_3 stores information due to its shape anisotropy, which was clarified by Stoner and Wohlfarth's work in 1948, and that is the reason why Stoner–Wohlfarth model is very important.

The effective anisotropy energy density of a Stoner–Wohlfarth single-domain particle is from the self-demagnetizing energy term as given in Eq. (2.51), where the self-demagnetizing matrix $\tilde{N}(\mathbf{r}, \mathbf{r})$ is diagonal, with $N_{11} = N_{22}$ and $N_{33} < N_{11}$ along its long-axis $\hat{k}_s$, due to the rotational symmetry of the elongated particle:

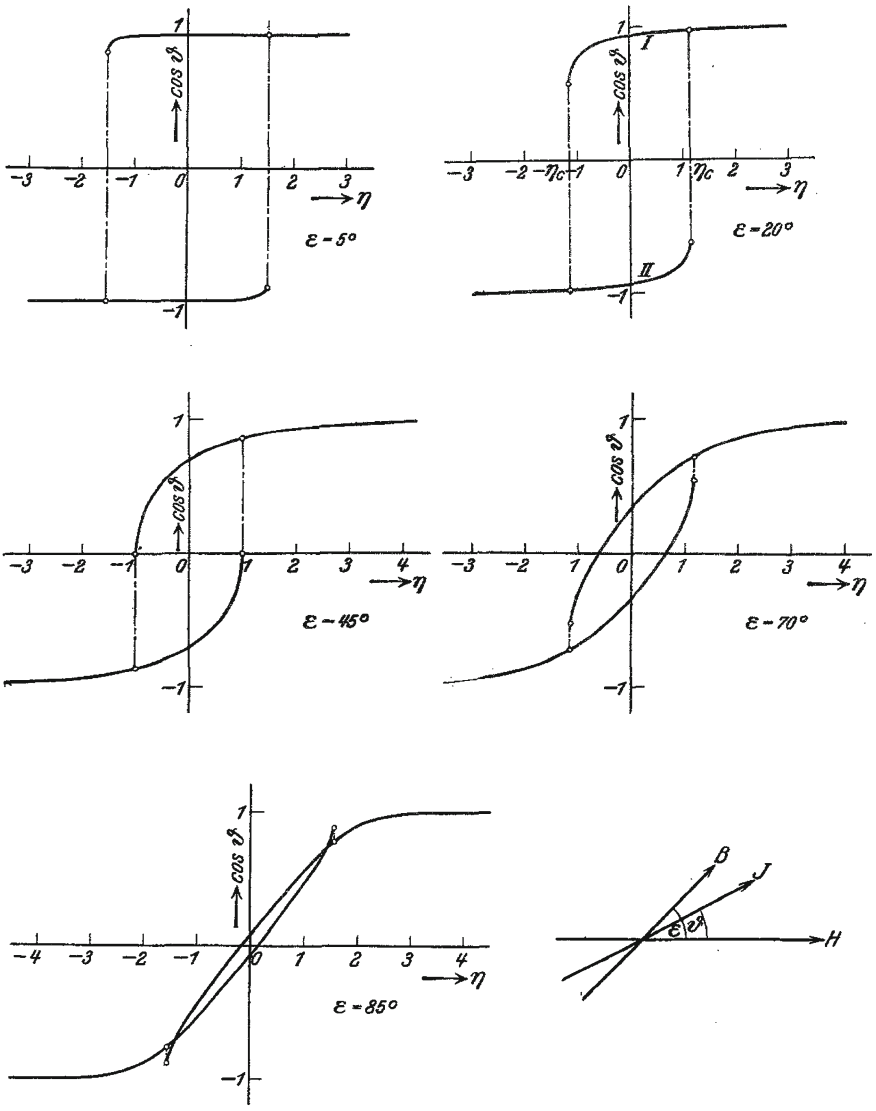

Fig. 2.8 M–H loops of an element with uniaxial anisotropy, where ε is the angle between the external field and the easy axis. © with kind permission from Springer Science and Business Media: [10], Fig. 3

$$\begin{aligned} \mathscr{E}/V &= \frac{1}{2}4\pi M_s^2\left(N_{11}m_1^2 + N_{22}m_2^2 + N_{33}m_3^2\right) - \mathbf{H}\cdot\mathbf{M} \\ &= \mathscr{E}_0 - \left[2\pi M_s^2(N_{11} - N_{33})\right](\hat{m}\cdot\hat{k}_s)^2 - \mathbf{H}\cdot\mathbf{M} \\ &= \mathscr{E}_0 - K_s\cos^2(\phi-\theta) - M_s H\cos\phi \end{aligned} \tag{2.71}$$

where the angle $\phi = \langle \mathbf{H}, \hat{m} \rangle$ and $\theta = \langle \mathbf{H}, \hat{k}_s \rangle$ of the Stoner–Wohlfarth model take the position of the angle θ and ε respectively in Eq. (2.70) and Fig. 2.8 of Becker's rigid rotational model. The shape anisotropy energy $K_s = 2\pi M_s^2(N_{11} - N_{33})$; thus the shape anisotropy field constant $H_k^s = 2K_s/M_s = 4\pi M_s(N_{11} - N_{33})$.

If we use the LL equations or the LLG equations to find the static or dynamic magnetic states, but not the energy minimization method like the Stoner–Wohlfarth model, the effective shape anisotropy field of an arbitrary shaped micromagnetic cell can be very simple and straightforward:

$$\begin{aligned} \mathscr{E}_a^s / V &= \frac{1}{2} 4\pi M_s^2 (m_1, m_2, m_3) \begin{pmatrix} N_{11} & N_{12} & N_{13} \\ N_{12} & N_{22} & N_{23} \\ N_{13} & N_{23} & N_{33} \end{pmatrix} \begin{pmatrix} m_1 \\ m_2 \\ m_3 \end{pmatrix} \qquad (2.72) \\ &= \frac{1}{2} 4\pi M_s^2 \left\{ (N_{11} - N_{33}) m_1^2 + (N_{22} - N_{33}) m_2^2 + N_{33} \right. \\ &\quad \left. + 2N_{12} m_1 m_2 + 2N_{13} m_1 \sqrt{1 - m_1^2 - m_2^2} + 2N_{23} m_2 \sqrt{1 - m_1^2 - m_2^2} \right\} \end{aligned}$$

$$-\mathbf{H}_k^s = \frac{\partial \mathscr{E}_a^s}{\partial (V M_s \hat{m})} = 4\pi M_s \begin{pmatrix} N_{11} & N_{12} & N_{13} \\ N_{12} & N_{22} & N_{23} \\ N_{13} & N_{23} & N_{33} \end{pmatrix} \begin{pmatrix} m_1 \\ m_2 \\ m_3 \end{pmatrix} - h_0\{\hat{m}\} \begin{pmatrix} m_1 \\ m_2 \\ m_3 \end{pmatrix} \qquad (2.73)$$

where $h_0\{\hat{m}\} = 4\pi M_s(m_1 N_{13} + m_2 N_{23} + m_3 N_{33})/m_3$ is a scalar. Thus, if we use LLG equations, after considering the constraint $\hat{m}^2 = 1$, the shape anisotropy field of an arbitrary cell in Eq. (2.73) is equivalent to the self-demagnetizing field term in the general expression of the magnetostatic interaction field in Eq. (2.60).

In 1970s, owing to the invention of personal computers, the computational methods were developed gradually to analyze media and heads in recording systems, although strictly speaking, "nanomagnetics" is a more suitable term.

In 1980s, two main computational micromagnetic methods were developed: finite difference method (FDM) and finite element method (FEM). The most important development of the computational magnetics was the inclusion of the magnetostatic energy in the micromagnetic model. In traditional domain theory, such as in Landau–Lifshitz's work, this term of magnetostatic energy was ignored [1]:

$$\mathscr{E} = \int \mathrm{d}V \left[\frac{1}{2} \alpha s'^2 + \frac{1}{2} \beta \left(s_x^2 + s_y^2 \right) \right], \quad \mathbf{s} = (0, s \sin\theta, s \cos\theta), \qquad (2.74)$$

$$\alpha\theta'' - \beta \sin\theta \cos\theta = 0 \quad \Rightarrow \quad \cos\theta = -\tanh[x/\sqrt{\alpha/\beta}] \qquad (2.75)$$

where the coefficient $\alpha = 2A^*$, $\beta = 2K_1$, and $s'^2 = \sum_i (\mathrm{d}s_i/\mathrm{d}x)(\mathrm{d}s_i/\mathrm{d}x)$. The boundary condition of the Bloch wall is $\theta = 0, \pi$ at $x = -\infty, +\infty$, respectively. The Bloch wall width $a = \sqrt{\alpha/\beta}$ equals the Bloch exchange length $l_{ex}^B = \sqrt{A^*/K_1}$. The ignore of magnetostatic energy was reasonable for the Bloch wall, because its magnetic pole density $-\nabla \cdot \mathbf{M}$ is zero. However, for most of other cases in

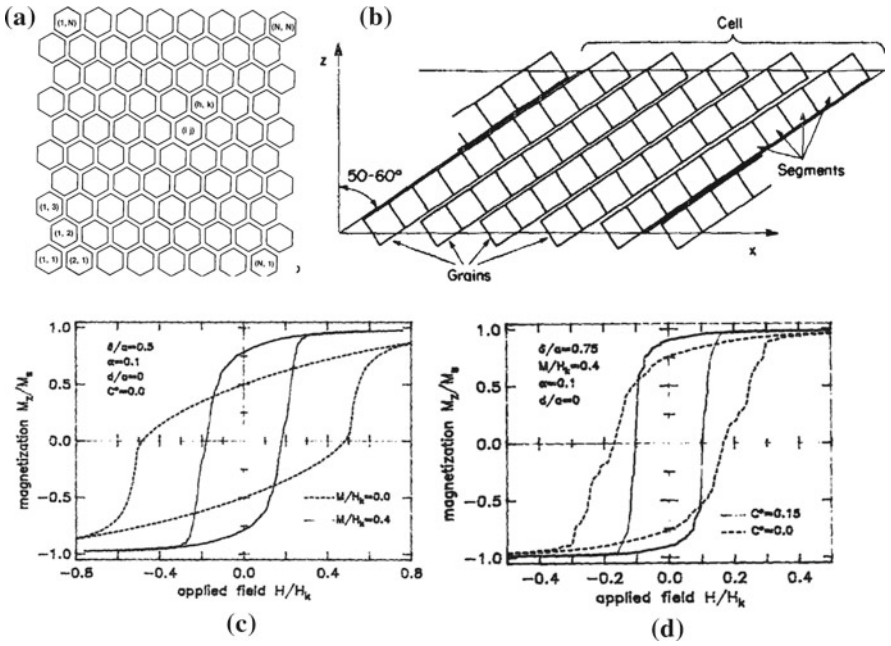

Fig. 2.9 FDM and FDM–FFT micromagnetic method. **a** Model of magnetic grains in Co–P thin film; © Reprinted with permission from Ref. [17]. Copyright [1983], American Institute of Physics; **b** model of micromagnetic cells in CoNi film; © Reprinted with permission from Ref. [18]. Copyright [1987], American Institute of Physics; **c**, **d** effects of magnetostatic interaction (M_s/H_k) and exchange interaction ($C^* = H_e/H_k$) among the grains on M–H loops using FDM–FFT method; © Reprinted with permission from Ref. [19]. Copyright [1988], American Institute of Physics

applied magnetism, this ignorance of the demagnetizing field is not correct, and the computational magnetics is necessary to include the term $\mathbf{H}_m$ in Eq. (2.60).

The FDM uses regular mesh of micromagnetic cells to discretize the magnetic material. In 1983, Hughes used the energy minimization method to calculate the M–H loops of Co–P thin film, where hexagonal grains arranged on a triangular lattice was chosen as the regular mesh, as seen in Fig. 2.9a [17]. In 1987, Victora used the LLG equations to calculate the torque curve of CoNi film, where the complete magnetostatic interaction was included for micromagnetic cells in Fig. 2.9b by a direct integration [18]. In 1988, Bertram and Zhu developed a FDM–FFT method for the micromagnetic model, where the computation of the magnetostatic interaction was largely speed up by using the fast-Fourier-transform (FFT) method [19]. By using FDM–FFT method, the effects of the magnetostatic interaction among all grains and the exchange among neighbor grains can be carefully studied, as seen in Fig. 2.9c, d, which was important for the development of low-noise thin film recording media. The Object-Oriented MicroMagnetic Framework (OOMMF) software of micromagnetics was initiated in the Intermag 1995, based on discussions of micromagnetic standard problems in Intermag 1994 and Intermag 1995. OOMMF uses FDM–FFT methods,

which is developed by NIST and widely utilized recently [20]. All micromagnetic studies in the following chapters of this book are accomplished by FDM–FFT or its improved version, as introduced in Sect. 2.2 of this chapter.

The FEM was initially proposed by Fredkin and Koehler in 1987 [21], where a 2-D thin film was discretized into triangle elements, and the energy minimization was taken with respect to the magnetization $\hat{m}$. The key path was to find the magnetic field energy from $\hat{m}$ defined at barycenters of triangular cells:

$$\begin{aligned} &\hat{m} \text{ at barycenter} \quad \Rightarrow \quad \text{vector potential } \mathbf{A} \text{ at vertex} \Rightarrow \\ &\mathbf{B} \text{ at barycenter} \quad \Rightarrow \quad \text{magnetic field energy } |\mathbf{B}|^2/8\pi \end{aligned} \tag{2.76}$$

The simulation speed and efficiency of FEM micromagnetics has been largely improved by Fidler and Schrefl [22] and Scholz [23], who worked at Vienna University of Technology, where the scalar magnetic potential but not the vector potential is the key to solve magnetostatic interactions [23]:

$$\nabla^2 \phi = 4\pi \nabla \cdot \mathbf{M} \qquad (\mathbf{M} = 0 \text{ outside magnetic domain } \Omega) \tag{2.77}$$

$$\phi_{\text{external}} = \phi_{\text{internal}} , \qquad \frac{\partial \phi_{\text{external}}}{\partial \hat{n}} - \frac{\partial \phi_{\text{internal}}}{\partial \hat{n}} = 4\pi \hat{n} \cdot \mathbf{M} \tag{2.78}$$

The Dirichilet boundary condition in Eq. (2.78) contains an approximation, which will be better in soft magnetic materials than in hard magnetic materials.

Appendix

Appendix A

If a $a' \times b'$ rectangle locates at $z' = 0$, and the observation position vector is located at $\mathbf{r} = (x, y, z) = (r_1, r_2, r_3)$, as seen in Fig. 2.4a, the three nonzero elements in the demagnetizing matrix of a rectangular surface are ($\alpha = 1, 3$):

$$N_{\alpha 3}^{\text{rec}}(\mathbf{r}) = -\frac{1}{4\pi} \int_{-a'/2}^{a'/2} \mathrm{d}r_1' \int_{-b'/2}^{b'/2} \mathrm{d}r_2' \frac{r_\alpha - r_\alpha'}{\left[(r_1 - r_1')^2 + (r_2 - r_2')^2 + r_3^2\right]^{3/2}} \tag{2.79}$$

We just have to do two integrations for N_{33}^{rec} and N_{13}^{rec}, and the integration of N_{23}^{rec} is totally analogy to N_{13}^{rec}. Let's start with N_{13}^{rec}:

$$
\begin{aligned}
N_{13}^{\mathrm{rec}} &= -\frac{1}{4\pi}\int_{-a'/2}^{a'/2}\mathrm{d}x'\int_{-b'/2}^{b'/2}\mathrm{d}y'\frac{x-x'}{\left[(x-x')^2+(y-y')^2+z^2\right]^{3/2}} \\
&= -\frac{1}{4\pi}\int_{-b'/2}^{b'/2}\mathrm{d}y'\left.\frac{1}{\left[(x-x')^2+(y-y')^2+z^2\right]^{1/2}}\right|_{x'=-a'/2}^{a'/2} \\
&= -\frac{1}{4\pi}\sum_q(-q)\ln\left(y'-y+\sqrt{R_1^2+(y-y')^2+R_3^2}\right)_{y'=-b'/2}^{b'/2} \\
&= -\frac{1}{4\pi}\sum_q\sum_w qw\ln\left(R-wR_2\right)
\end{aligned}
\tag{2.80}
$$

The variables are defined in Table 2.2. The integration for N_{33}^{rec} can also be done:

$$
\begin{aligned}
N_{33}^{\mathrm{rec}} &= -\frac{1}{4\pi}\int_{-a'/2}^{a'/2}\mathrm{d}x'\int_{-b'/2}^{b'/2}\mathrm{d}y'\frac{z}{\left[(x-x')^2+(y-y')^2+z^2\right]^{3/2}} \\
&= -\frac{1}{4\pi}\int_{-b'/2}^{b'/2}\mathrm{d}y'\frac{z}{\left[(y-y')^2+z^2\right]}\left.\frac{x'-x}{\left[(x-x')^2+(y-y')^2+z^2\right]^{1/2}}\right|_{x'=-a'/2}^{a'/2} \\
&= -\frac{1}{4\pi}\sum_q\arctan\left(\frac{R_1}{R_3}\frac{y'-y}{\sqrt{R_1^2+(y-y')^2+R_3^2}}\right)\Bigg|_{y'=-b'/2}^{b'/2} \\
&= -\frac{1}{4\pi}\sum_q\sum_w\arctan\frac{R_1R_2}{R_3R}
\end{aligned}
\tag{2.81}
$$

The $N_{\alpha3}^{\mathrm{rec}}(\mathbf{r})$ of a rectangular surface have be listed in Table 2.2 respectively.

Appendix B

If the surface located at $z'=0$ is a right-angle triangle with right-angle side lengths (a', b'), the origin at the midpoint of the hypotenuse, and the hypotenuse defined by equation $y'=-sx'$ or $x'=-vy'$, and the observation position vector is located at $\mathbf{r}=(x,y,z)$, there are still three nonzero elements N_{13}^{tri}, N_{23}^{tri} and N_{33}^{tri} in the demagnetizing matrix of a triangular surface, as seen in Fig. 2.4b. Here we can first do the integral for element N_{13}^{tri}:

$$
\begin{aligned}
N_{13}^{\mathrm{tri}} &= -\frac{1}{4\pi}\int_{-b'/2}^{b'/2}\mathrm{d}y'\int_{-vy'}^{a'/2}\mathrm{d}x'\frac{x-x'}{\left[(x-x')^2+(y-y')^2+z^2\right]^{3/2}} \\
&= -\frac{1}{4\pi}\int_{-b'/2}^{b'/2}\mathrm{d}y'\left\{\frac{1}{\left[(a'/2-x)^2+(y-y')^2+z^2\right]^{1/2}}\right. \\
&\qquad\left. -\frac{1}{\left[(x+vy')^2+(y-y')^2+z^2\right]^{1/2}}\right\} \\
&= -\frac{1}{4\pi}\ln\left(y'-y+\sqrt{(a'/2-x)^2+(y-y')^2+z^2}\right)\Big|_{y'=-b'/2}^{b'/2} \\
&\quad +\frac{1}{4\pi}\int_{-b'/2}^{b'/2}\mathrm{d}y'\frac{1}{\sqrt{1+v^2}}\frac{1}{\left[(y'-c_1)^2+r^2/(1+v^2)-c_1^2\right]^{1/2}} \\
&= \frac{1}{4\pi}\sum_w w\ln\left(R_{\mathrm{I}}-wR_2\right) \\
&\quad +\frac{1}{4\pi}\frac{1}{\sqrt{1+v^2}}\ln\left(y'-c_1+\sqrt{(y'-c_1)^2+c_2^2}\right)\Big|_{y'=-b'/2}^{b'/2} \\
&= -\frac{1}{4\pi}\sum_w w\left\{\frac{1}{\sqrt{1+v^2}}\ln(P-wP_2)-\ln(R_{\mathrm{I}}-wR_2)\right\}
\end{aligned}
\tag{2.82}
$$

The symbols $c_1, c_2^2, P, P_2, R_{\mathrm{I}}$, and R_2 used in Eq. (2.82) have be defined in Tables 2.2 and 2.3 respectively. The integration for N_{23}^{tri} is totally analogy to N_{13}^{tri}, just with a $x \leftrightarrow y$ symmetry, therefore the derivation of N_{23}^{tri} will be omitted here.

The integral for the matrix element N_{33}^{tri} is the most complicated one, which include three parts:

$$
\begin{aligned}
N_{33}^{\mathrm{tri}} &= -\frac{1}{4\pi}\int_{-b'/2}^{b'/2}\mathrm{d}y'\int_{-vy'}^{a'/2}\mathrm{d}x'\frac{z}{\left[(x-x')^2+(y-y')^2+z^2\right]^{3/2}} \\
&= -\frac{1}{4\pi}\int_{-b'/2}^{b'/2}\mathrm{d}y'\,\frac{z}{\left[(y-y')^2+z^2\right]}\frac{x'-x}{\left[(x-x')^2+(y-y')^2+z^2\right]^{1/2}}\Bigg|_{x'=-vy'}^{a'/2} \\
&= -\frac{1}{4\pi}\left\{N_{33}^{(1)}+N_{33}^{(2)}+N_{33}^{(3)}\right\}
\end{aligned}
\tag{2.83}
$$

In Eq. (2.83), the derivation of the first term $N_{33}^{(1)}$ is actually very similar to one of the two terms in Eq. (2.81) for rectangular surface; in the second term, the numerator of

the integrand is $z(-vy'-x)$, which can be disassembled into two parts $zv(-y'+y)$ and $z(-vy-x)$, and these two part just corresponds to the $N_{33}^{(2)}$ and $N_{33}^{(3)}$ respectively.

The integration for $N_{33}^{(1)}$ is just straightforward:

$$\begin{aligned} N_{33}^{(1)} &= \int_{-b'/2}^{b'/2} \mathrm{d}y' \frac{z}{\left[(y-y')^2+z^2\right]} \frac{a'/2-x}{\left[(a'/2-x)^2+(y-y')^2+z^2\right]^{1/2}} \\ &= \arctan\left(\frac{a'/2-x}{z} \frac{y'-y}{\sqrt{(a'/2-x)^2+(y-y')^2+z^2}} \right)\Bigg|_{y'=-b'/2}^{b'/2} \\ &= \sum_w \arctan[(a'/2-x)R_2/(zR_\mathrm{I})] \end{aligned} \tag{2.84}$$

In the derivation for $N_{33}^{(2)}$, complicated variables such as c_1, c_2 and $c_5 = y - \mathrm{i}z$ in Table 2.3 have to be defined, and the respective integral is:

$$\begin{aligned} N_{33}^{(2)} &= \int_{-b'/2}^{b'/2} \mathrm{d}y' \frac{zv}{\left[(y-y')^2+z^2\right]} \frac{y'-y}{\left[(x+vy')^2+(y-y')^2+z^2\right]^{1/2}} \\ &= \int_{-b'/2}^{b'/2} \mathrm{d}y' \frac{zv}{2} \left[\frac{1}{y'-c_5} + \frac{1}{y'-c_5^*} \right] \frac{1}{\sqrt{1+v^2}} \frac{1}{\left[(y'-c_1)^2+c_2^2\right]^{1/2}} \end{aligned} \tag{2.85}$$

The previous integration include two terms which are complex conjugates of one another. Now let's make an integration variable change $y' - c_1 = c_2 \sinh\theta$ with the two integration limits of the angle θ as $\theta_1 = \sinh^{-1}[(-b'/2 - c_1)/c_2]$ and $\theta_2 = \sinh^{-1}[(b'/2 - c_1)/c_2]$, the integral in Eq. (2.85) has the form:

$$N_{33}^{(2)} = \frac{zv}{2\sqrt{1+v^2}} \int_{\theta_1}^{\theta_2} \left[\frac{\mathrm{d}\theta}{c_1 - c_5 + c_2 \sinh\theta} + c.c. \right] \tag{2.86}$$

Then make another variable change $e^\theta = u$, and define a new constant $\sinh\eta = (c_1 - c_5)/c_2$, the integral becomes:

$$
\begin{aligned}
N_{33}^{(2)} &= \frac{zv}{\sqrt{1+v^2}} \int_{u_1}^{u_2} \left[\frac{1}{c_2} \frac{\mathrm{d}\left(e^{\theta}\right)}{\left(e^{\theta}\right)^2 + 2[(c_1-c_5)/c_2]e^{\theta} - 1} + c.c. \right] \\
&= \frac{zv}{\sqrt{1+v^2}} \int_{u_1}^{u_2} \left[\frac{1}{c_2} \frac{\mathrm{d}u}{(u+e^{\eta})(u-e^{-\eta})} + c.c. \right] \\
&= \frac{zv}{\sqrt{1+v^2}} \left\{ \frac{1}{2c_2 \cosh\eta} \ln \frac{u-e^{-\eta}}{u+e^{\eta}} \Big|_{u=u_1}^{u_2} + c.c. \right\} \\
&= \frac{zv}{\sqrt{1+v^2}} \sum_{w} \Re \left\{ \frac{w}{\sqrt{(c_1-c_5)^2+c_2^2}} \ln \frac{V_+}{V_-} \right\} \\
&= \frac{zv}{\sqrt{1+v^2}} \sum_{w} \Re \left\{ \frac{w}{Ae^{\mathrm{i}\theta'/2}} \ln \frac{|V_+|e^{\mathrm{i}\phi_+}}{|V_-|e^{\mathrm{i}\phi_-}} \right\}
\end{aligned} \tag{2.87}
$$

In the previous derivation, the difficult part is to find integration limits u_1 and u_2. Actually $\sinh^{-1} x = \ln[x + \sqrt{x^2+1}]$, therefore u_1, u_2, e^{η} and $e^{-\eta}$ are:

$$
\begin{aligned}
u_1 = e^{\theta_1} &= \frac{1}{c_2} \left[-\left(\frac{b'}{2} + c_1\right) + \sqrt{\left(\frac{b'}{2} + c_1\right)^2 + c_2^2} \right] \\
u_2 = e^{\theta_2} &= \frac{1}{c_2} \left[+\left(\frac{b'}{2} - c_1\right) + \sqrt{\left(\frac{b'}{2} - c_1\right)^2 + c_2^2} \right] \\
e^{\eta} &= \frac{1}{c_2} \left[+(c_1-c_5) + \sqrt{(c_1-c_5)^2 + c_2^2} \right] \\
e^{-\eta} &= \frac{1}{c_2} \left[-(c_1-c_5) + \sqrt{(c_1-c_5)^2 + c_2^2} \right]
\end{aligned} \tag{2.88}
$$

By defining $P_2 = \frac{b'}{2} + wc_1$ ($w = +1$ and $w = -1$ are for the two integral limits u_1 and u_2 respectively), $Ae^{\mathrm{i}\theta'/2}$, V_+ and V_- will have the forms in Table 2.3:

$$
\frac{u-e^{-\eta}}{u+e^{\eta}} = \frac{-wP_2 + \sqrt{P_2^2+c_2^2} + (c_1-c_5) - \sqrt{(c_1-c_5)^2+c_2^2}}{-wP_2 + \sqrt{P_2^2+c_2^2} + (c_1-c_5) + \sqrt{(c_1-c_5)^2+c_2^2}} = \frac{V_-}{V_+} \tag{2.89}
$$

The integration of $N_{33}^{(3)}$ is similar to $N_{33}^{(2)}$, which also includes imaginary numbers:

$$N_{33}^{(3)} = \int_{-b'/2}^{b'/2} \mathrm{d}y' \frac{z}{\left[(y-y')^2+z^2\right]} \frac{x+vy}{\left[(x+vy')^2+(y-y')^2+z^2\right]^{1/2}} \tag{2.90}$$

$$= \int_{-b'/2}^{b'/2} \mathrm{d}y' \frac{x+vy}{2\mathrm{i}} \left[\frac{-1}{y'-c_5} + \frac{1}{y'-c_5^*}\right] \frac{1}{\sqrt{1+v^2}} \frac{1}{\left[(y'-c_1)^2+c_2^2\right]^{1/2}}$$

The rest of derivations are similar to Eq. (2.87), but the result is an imaginary part:

$$\begin{aligned} N_{33}^{(3)} &= -\frac{x+vy}{2\mathrm{i}\sqrt{1+v^2}} \int_{\theta_1}^{\theta_2} \left[\frac{\mathrm{d}\theta}{c_1-c_5+c_2\sinh\theta} - c.c.\right] \\ &= -\frac{x+vy}{2\mathrm{i}\sqrt{1+v^2}} \int_{u_1}^{u_2} \left[\frac{1}{c_2}\frac{\mathrm{d}u}{(u+e^{\eta})(u-e^{-\eta})} - c.c.\right] \\ &= -\frac{x+vy}{\sqrt{1+v^2}} \sum_w \Im\left\{\frac{w}{\sqrt{(c_1-c_5)^2+c_2^2}} \ln\frac{V_+}{V_-}\right\} \\ &= -\frac{x+vy}{\sqrt{1+v^2}} \sum_w \Im\left\{\frac{w}{Ae^{\mathrm{i}\theta'/2}} \ln\frac{|V_+|e^{\mathrm{i}\phi_+}}{|V_-|e^{\mathrm{i}\phi_-}}\right\} \end{aligned} \tag{2.91}$$

Finally, insert the results of the three parts in Eqs. (2.84), (2.87) and (2.91) into Eq. (2.81), the most difficult matrix element of a triangular surface N_{33}^{tri} can be found.

References

1. Landau, L.D., Lifshitz, E.: Electrodynamics of Continuous Media, translated from Russian by Sykes J.B. and Bell J.S. Pergamon Press, Oxford (1960)
2. Brown, W.F., Jr., La Bonte, A.E.: Structure and energy of one-dimensional domain walls in ferromagnetic thin films. J. Appl. Phys. **36**(4), 1380–1386 (1965)
3. Maxwell J.C.: A Treatise on Electricity and Magnetism (1873), translated by Ge G. into Chinese. Wuhan Press, Wuhan (1994)
4. von Laue M.: Geschichte der Physik (1950), translated by Fan D. N. and Dai N.Z. into Chinese. Commercial Press, Beijing (1978)
5. Wei, D., Wang, S.M., Ding, Z.J., Gao, K.Z.: Micromagnetics of ferromagnetic nano-devices using fast fourier transform method. IEEE Trans. Magn. **45**(8), 3035–3045 (2009)
6. Schabes, M.E., Aharoni, A.: Magnetostatic interaction fields for a three-dimensional array of ferromagnetic cubes. IEEE Trans. Magn. **23**(6), 3882–3888 (1987)
7. Wei, D.: Fundamentals of Electric, Magnetic, Optic Materials and Devices (in chinese), 2nd edn. Science Press, Beijing (2009)

8. Landau, L.D., Lifshitz, E.: On the theory of the dispersion of magnetic permeability in ferromagnetic bodies. Phys. Zeitsch. der Sow. **8**, 153 (1935), reprinted in English by Ukr. J. Phys. **53**, 14 (2008)
9. Akulov, N.S.: Zur atomtheorie des ferromagnetismus. Z. Phys. **54**, 582–587 (1929)
10. Becker, R.: Zur theorie der magnetisierungskurve. Z. Phys. **62**, 253–269 (1930)
11. Bloch, F.: Zur theorie des Austauschproblems und der Remanenzerscheinung der ferromagnetika. Z. Phys. **74**, 295–335 (1932)
12. Gilbert, T.L.: A phenomenological theory of damping in ferromagnetic materials. IEEE Trans. Magn. **40**(6), 3443–3449 (2004)
13. Brown, W.F., Jr.: Micromagnetics. Wiley, New York (1963)
14. Kaya, S.: On the magnetization of single crystals of nickel, vol. 17, p. 1157. Science Report, Tohoku University (1928)
15. Stoner, E.C., Wohlfarth, E.P.: A mechanism of magnetic hysteresis in heterogeneous alloys. IEEE Trans. Magn. **27**(4), 3475–3518 (1991)
16. Stoner, E.C., Wohlfarth, E.P.: A mechanism of magnetic hysteresis in heterogeneous alloys. Philos. Trans. R. Soc. Lond. A **240**, 599 (1948)
17. Hughes, G.F.: Magnetization reversal in cobalt-phosphorus films. J. Appl. Phys. **54**, 5306–5313 (1983)
18. Victora, R.H.: Micromagnetic predictions for magnetization reversal in CoNi films. J. Appl. Phys. **62**, 4220–4225 (1987)
19. Bertram, H.N., Zhu, J.G.: Micromagnetic studies of thin metallic films. J. Appl. Phys. **63**, 3248–3253 (1988)
20. NIST: Object Oriented MicroMagnetic Framework (OOMMF) Project. NIST Center for Information Technology Laboratory. http://www.math.nist.gov/oommf/ (2006). Accessed 20 June 2011
21. Fredkin, D.R., Koehler, T.R.: Numerical micromagnetics by the finite element method. IEEE Trans. Magn. **23**(5), 3385–3387 (1987)
22. Fidler, J., Schrefl, T.: Micromagnetic modelling—the current state of the art. J. Phys. D Appl. Phys. **33**, R135–R156 (2000)
23. Scholz, W., Fidler, J., Schrefl, T., Suess, D., Dittrich, R., Forster, H., Tsiantos, V.: Scalable parallel micromagnetic solvers for magnetic nanostructures. Comput. Mater. Sci. **28**, 366–383 (2003)